NACA TN No. 1630

NATIONAL ADVISORY COMMITTEE FOR AERONAUTICS

TECHNICAL NOTE

No. 1630

A GENERALIZED THEORETICAL INVESTIGATION OF THE HYDRODYNAMIC PITCHING MOMENTS EXPERIENCED BY V-BOTTOM SEAPLANES DURING STEP-LANDING IMPACTS AND COMPARISONS WITH EXPERIMENT

By Benjamin Milwitzky

Langley Memorial Aeronautical Laboratory
Langley Field, Va.

LIBRARY COPY
JUN 16 1955
LANGLEY AERONAUTICAL LABORATORY
LIBRARY, NACA
LANGLEY FIELD, VIRGINIA

Washington
June 1948

THIS DOCUMENT ON LOAN FROM THE FILES OF

NATIONAL ADVISORY COMMITTEE FOR AERONAUTICS
LANGLEY MEMORIAL AERONAUTICAL LABORATORY
LANGLEY FIELD, HAMPTON, VIRGINIA

RETURN TO THE ABOVE ADDRESS.

REQUESTS FOR PUBLICATIONS SHOULD BE ADDRESSED AS FOLLOWS:

NATIONAL ADVISORY COMMITTEE FOR AERONAUTICS
1724 F STREET, N.W.,
WASHINGTON 25, D.C.

THIS DOCUMENT ON LOAN FROM THE FILES OF

NATIONAL ADVISORY COMMITTEE FOR AERONAUTICS
LANGLEY MEMORIAL AERONAUTICAL LABORATORY
LANGLEY FIELD, HAMPTON, VIRGINIA

RETURN TO THE ABOVE ADDRESS.

REQUESTS FOR PUBLICATIONS SHOULD BE ADDRESSED AS FOLLOWS:

NATIONAL ADVISORY COMMITTEE FOR AERONAUTICS
1724 F STREET, N.W.,
WASHINGTON 25, D.C.

NATIONAL ADVISORY COMMITTEE FOR AERONAUTICS

TECHNICAL NOTE NO. 1630

A GENERALIZED THEORETICAL INVESTIGATION OF THE HYDRODYNAMIC PITCHING MOMENTS EXPERIENCED BY V-BOTTOM SEAPLANES DURING STEP-LANDING IMPACTS AND COMPARISONS WITH EXPERIMENT

By Benjamin Milwitzky

SUMMARY

A theoretical investigation is made of the hydrodynamic pitching moments experienced by V-bottom seaplanes during step-landing impacts. The entire immersion process is analyzed from the instant of initial contact until the seaplane rebounds from the water surface. In the analysis the primary flow about the immersed portion of a keeled float or hull is considered to occur in transverse flow planes and the virtual-mass concept is applied to calculate the reaction of the water to the motion of the seaplane.

It is shown that the pitching moment and the center-of-pressure location may be represented in generalized form by means of dimensionless variables which take into account the effects of such factors as the seaplane weight, angle of dead rise, trim angle, and initial velocity. The variation of these coefficients during an impact is governed by the magnitude of a single parameter, called the approach parameter κ, that is determined by the trim and the initial flight-path angle and permits reduction of the impact variables to a common basis.

Equations are presented from which the variation of the pitching-moment and center-of-pressure coefficients have been calculated for a wide range of conditions extending from impacts along shallow flight paths approaching planing to very steep impacts where the resultant velocity is normal to the keel. Solutions are also presented for the conditions which exist at the instants of maximum acceleration, maximum moment, maximum draft, and at the instant of zero draft during rebound. The results show that the maximum hydrodynamic pitching moment is attained slightly after the maximum acceleration is reached and occurs prior to the attainment of the maximum draft.

The analysis also shows that the pitching moment about the step at any given stage of the impact process is independent of the angle of dead rise and that the center of pressure in an impact is located at a

distance only slightly greater than one-third the wetted length forward of the step. The most forward center-of-pressure locations, in terms of the wetted length, are attained at low values of the approach parameter κ (which, for a given trim angle, correspond to steep flight paths) but the center-of-pressure distance converges to a limiting value of exactly one-third the wetted length forward of the step as the planing condition is approached.

Comparisons of theoretical pitching-moment time histories and maximum values of the pitching moment with experimental data obtained in the Langley impact basin with floats of 30° and 40° angles of dead rise indicate that the calculated results are in good agreement with the measured values.

INTRODUCTION

Because of the evident need for a more rational foundation upon which to base water-loading requirements for the design of modern seaplanes, an extensive theoretical and experimental research program has been undertaken in the field of hydrodynamic impact loads. The theoretical phase of the program has resulted in references 1 and 2, which deal with the analysis of impact loads for V-bottom seaplanes. Reference 1 presents a critical survey of previously published impact theories, which are shown to be applicable only to impacts where the resultant velocity is normal to the keel, and in addition considers the effect of the velocity component parallel to the keel. Reference 2 provides a generalized analysis, with experimental confirmation, of the motions and overall hydrodynamic loads experienced by V-bottom seaplanes throughout the course of step-landing impacts and shows that the motion and time characteristics of such impacts may be represented by means of dimensionless variables which take into account such factors as the seaplane weight, dead-rise angle, trim angle, and initial velocity. The variation of these coefficients during an impact was shown to be governed solely by the magnitude of a single parameter, called the approach parameter κ, which is determined by the trim and the flight-path angle at the instant of initial contact with the water surface.

The present paper represents a continuation of the work of reference 2 and applies the theoretical coefficients and equations introduced by that paper to the development of the nondimensional hydrodynamic pitching-moment and center-of-pressure coefficients for step-landing impacts. The entire immersion process is analyzed from the instant of initial contact until the seaplane rebounds from the water surface. In the analysis the primary flow about the immersed portion of a keeled seaplane float is considered to occur in transverse flow planes and the virtual-mass concept is applied to calculate the reaction of the water

to the motion of the seaplane. The results of the analysis are presented in the form of charts which may be used to determine the hydrodynamic pitching moments and the center-of-pressure location on a seaplane at any time during an impact as well as the pitching moments, the center-of-pressure location, the state of motion of the seaplane, and the time after contact at the particular instants of maximum pitching moment, maximum acceleration, maximum draft, and at the instant of zero draft during rebound. The applicability of the theoretical results is illustrated by comparisons with experimental data obtained in the Langley impact basin with a V-bottom float (fig. 1) having an angle of dead rise of 30° at the step and a similar float of 40° angle of dead rise.

SYMBOLS

A	hydrodynamic aspect ratio
a	longitudinal distance between step and center of moments
b	longitudinal distance between center of gravity and center of moments
c	distance, measured normal to longitudinal axis, between center of gravity and center of moments
F	force
g	acceleration due to gravity
l	wetted keel length
M	pitching moment
m_w	two-dimensional virtual mass
n_{1_w}	impact load factor, measured normal to water surface $\left(-\frac{\ddot{y}}{g}\right)$
p	longitudinal distance between step and center of pressure
s	distance from given flow plane to foremost immersed station along keel
t	time after contact
V	velocity of seaplane
W	weight of seaplane or total testing weight
x	distance parallel to water surface

y	draft of keel at step, normal to water surface
z	penetration of a given station, normal to keel
β	angle of dead rise
γ	flight-path angle relative to water surface
ρ	mass density of water
τ	trim angle
$f(\beta)$	function governing variation of virtual mass with dead rise
$\phi(A)$	end-flow correction to total hydrodynamic load
$\phi_1(A)$	end-flow correction to hydrodynamic pitching moment

Subscripts:

f	float
h	horizontal or hydrodynamic
max	maximum
o	initial conditions or referring to point o
r	resultant
s	at the step
T	total
v	vertical

Dimensionless Variables

Pitching-moment coefficient based on vertical velocity

$$C_{m_s} = \frac{M_s}{\dot{y}_o^2} \left(\frac{g}{W}\right) \frac{\phi(A)}{\phi_1(A)} \sin \tau \cos \tau$$

Pitching-moment coefficient based on resultant velocity

$$C_{m_s}' = \frac{M_s}{V_{r_o}^{\ 2}} \left(\frac{g}{W}\right) \frac{\phi(A)}{\phi_1(A)}$$

Center-of-pressure coefficient

$$C_{cp} = p \sin \tau \frac{\phi(A)}{\phi_1(A)} \left(\frac{g}{W} \left\{\frac{\left[f(\beta)\right]^2 \phi(A) \rho \pi}{6 \sin \tau \cos^2 \tau}\right\}\right)^{1/3}$$

Ratio of center-of-pressure distance to wetted length

$$C_r = \frac{p}{l} \frac{\phi(A)}{\phi_1(A)}$$

Load-factor coefficient

$$C_l = \frac{n_{i_w} g}{\dot{y}_o^{\ 2}} \left(\frac{W}{g} \left\{\frac{6 \sin \tau \cos^2 \tau}{\left[f(\beta)\right]^2 \phi(A) \rho \pi}\right\}\right)^{1/3}$$

Vertical-velocity ratio

$$\frac{\dot{y}}{\dot{y}_o}$$

Draft coefficient

$$C_d = y \left(\frac{g}{W} \left\{\frac{\left[f(\beta)\right]^2 \phi(A) \rho \pi}{6 \sin \tau \cos^2 \tau}\right\}\right)^{1/3}$$

Time coefficient

$$C_t = t\dot{y}_o \left(\frac{g}{W} \left\{ \frac{\left[f(\beta)\right]^2 \phi(A) \rho \pi}{6 \sin \tau \cos^2 \tau} \right\} \right)^{1/3}$$

Approach parameter

$$\kappa = \frac{\sin \tau}{\sin \gamma_o} \cos (\tau + \gamma_o)$$

ANALYSIS

Basis of Analysis

A detailed discussion of the physical concepts upon which the analysis is based is given in references 1 and 2. Briefly, the flow about a slender immersing shape such as a keeled seaplane float or hull is assumed to occur in transverse flow planes which may be considered fixed in space and oriented normal to the keel. (See fig. 2.) Because of the absence of a satisfactory three-dimensional theory, the motion of the fluid in each flow plane is treated as a two-dimensional phenomenon. In order to account for the effects of end flow that exist in the three-dimensional case, the total force on the seaplane, which is obtained by integrating the reactions of the individual flow planes in contact with the hull, is reduced by the application of an aspect-ratio type of correction.

In any flow plane the momentum imparted to the water is determined solely by the growth of the float cross-sectional shape intersected by the plane and may be expressed as the product of the virtual mass associated with the immersed cross section and the velocity of penetration into the plane. After the step has passed through a given flow plane the intersected cross section ceases to exist and the plane becomes part of the downwash where it remains thereafter, independent of the subsequent progress of the impact.

In potential flow the two-dimensional virtual mass of any float cross section is determined by the shape immersed in the flow plane. In the case of V-shaped cross sections, if the chines are not immersed, the flow patterns at all degrees of penetration are models of each other

and the virtual mass is proportional to the square of the penetration. The constant of proportionality is determined by the dead-rise angle β. Thus the two-dimensional virtual mass of any V-shaped cross section may be expressed by

$$m_w = \left[f(\beta)\right]^2 \frac{\rho\pi}{2} z^2 \tag{1}$$

where the quantity $f(\beta)z$ represents the radius of an equivalent semi-cylinder of water constituting the virtual mass of the immersing shape.

On a two-dimensional basis, the momentum of the water contained within any flow plane is

$$m_w\dot{z} = \left[f(\beta)\right]^2 \frac{\rho\pi}{2} z^2\dot{z} \tag{2}$$

The reaction of the water within the plane is therefore given by

$$F = \left[f(\beta)\right]^2 \frac{\rho\pi}{2} \left(z^2\ddot{z} + 2z\dot{z}^2\right) \tag{3}$$

The total force on the seaplane, which acts normal to the keel, is obtained by integrating the forces contributed by the individual flow planes in contact with the hull. Since conventional floats and hulls are essentially prismatic for an appreciable distance forward of the step, the integration is performed under the assumption that the immersed portion of the hull has constant cross section and that the trim remains constant during the short duration of the impact; this integration gives

$$F_T = \left[f(\beta)\right]^2\phi(A) \frac{\rho\pi}{2 \tan \tau} \left(\frac{z_s{}^3\ddot{z}}{3} + z_s{}^2\dot{z}^2\right) \tag{4}$$

where the quantity $\phi(A)$ is applied to the calculated total force as a correction for the effects of end flow which exist in the three-dimensional case and is determined by the geometry of the immersed portion of the seaplane.

In reference 2 an analysis of the equations of motion resulting from the application of equation (4) to the condition where the wing lift is equal to the weight of the seaplane showed that the motion and time characteristics of such impacts may be represented in generalized form by means of the following dimensionless variables:

Load-factor coefficient

$$C_l = \frac{n_{i_w} g}{\dot{y}_o^{\,2}} \left(\frac{W}{g} \left\{ \frac{6 \sin \tau \cos^2 \tau}{\left[f(\beta)\right]^2 \phi(A) \rho \pi} \right\} \right)^{1/3} \tag{5}$$

where

$$n_{i_w} = -\frac{\ddot{y}}{g}$$

Draft coefficient

$$C_d = y \left(\frac{g}{W} \left\{ \frac{\left[f(\beta)\right]^2 \phi(A) \rho \pi}{6 \sin \tau \cos^2 \tau} \right\} \right)^{1/3} \tag{6}$$

Time coefficient

$$C_t = t\dot{y}_o \left(\frac{g}{W} \left\{ \frac{\left[f(\beta)\right]^2 \phi(A) \rho \pi}{6 \sin \tau \cos^2 \tau} \right\} \right)^{1/3} \tag{7}$$

Vertical-velocity ratio

$$\frac{\dot{y}}{\dot{y}_o} \tag{8}$$

It was also shown that the variation of these nondimensional quantities during the course of an impact is governed solely by the magnitude of the approach parameter

$$\kappa = \frac{\sin \tau}{\sin \gamma_o} \cos (\tau + \gamma_o) \tag{9}$$

which may be considered a criterion of impact similarity and depends only on the trim and the flight-path angle at the instant of initial contact.

For a given value of κ, therefore, the respective variations of the preceding dimensionless variables during an impact may each be represented by a single curve, regardless of what the dead-rise angle or weight of the seaplane, the attitude, or initial velocity may be. Similarly, there is a single variation with κ of each of the dimensionless variables representing the state of motion and the time at any given stage of the impact. Figure 3 is a graph of equation (9) and shows the variation of κ with trim and flight-path angle.

In the present analysis the theoretical coefficients and equations presented in reference 2 are applied in the development of the non-dimensional pitching-moment and center-of-pressure coefficients. As a result of this generalized treatment, the number of independent variables and the number of cases for which solutions are required are considerably reduced while the presentation and correlation of data for the entire range of seaplane and flight parameters is greatly simplified.

Although the application of the theoretical results to impacts of particular seaplanes requires the definition of $f(\beta)$ and $\phi(A)$, the generalized solutions of the motion and time characteristics of step landings in terms of the foregoing dimensionless variables are valid regardless of how these functions may be defined. The function $f(\beta)$, which governs the variation of virtual mass with dead rise, has been evaluated from the results of an iterative solution for the force on a two-dimensional V-shape immersing with constant velocity, reported by Wagner in reference 3. This variation is given by

$$f(\beta) = \frac{\pi}{2\beta} - 1 \tag{10}$$

The end-loss correction $\phi(A)$ may be approximated from the results of tests conducted by Pabst with vibrating plates in water (reference 4). Application of these results to the V-bottom seaplane gives

$$\phi(A) = 1 - \frac{\tan \tau}{2 \tan \beta} \tag{11}$$

Although the validity of the relationships given by equations (10) and (11) has not been experimentally verified for very low dead-rise angles, the application of these functions has yielded calculated results that closely agree with extensive test data obtained in the Langley impact basin with floats of $22\frac{1}{2}^{\circ}$, 30°, and 40° angles of dead rise and reported in references 1, 2, and 5.

Pitching Moments

As shown by equation (3), the force contributed by a given flow plane may be considered to arise from two sources: namely, the inertia reaction to the acceleration of the virtual mass and the additional change in momentum accompanying the expansion of the virtual mass with penetration into the flow planes. Under the assumption of two-dimensional flow within the flow planes, for a prismatic hull at positive trim, the inertia reaction follows a quadratic variation along the keel while the force due to the expansion of the virtual mass is linearly distributed. (See fig. 2.) The shape of the longitudinal distribution of the total force during an impact is, of course, determined by the relative magnitudes of the component distributions. For steady-state planing, however, since there is no acceleration, the total load is linearly distributed along the keel and the center of pressure is located at a distance equal to one-third the wetted length forward of the step.

Under actual three-dimensional conditions, however, as a result of the longitudinal components of flow introduced by the pressure gradient along the keel and the finite length, the theoretical two-dimensional distributions are somewhat modified as qualitatively shown in figure 2 by the broken-line curves, so that

$$F = \left[f(\beta)\right]^2 \frac{\rho\pi}{2} \left[f_1(A,s)z^2\ddot{z} + 2f_2(A,s)z\dot{z}^2\right]$$

where the reduction in force from that calculated by the assumption of two-dimensional flow in the flow planes is determined by the geometry of the immersed part of the hull and the station under consideration.

As a result of this effect the total load on the seaplane was reduced by the application of an aspect-ratio type of correction $\phi(A)$ which depends on the immersed shape of the hull. In the present analysis a similar type of reduction $\phi_1(A)$ is applied to the moments calculated by assuming two-dimensional flow in the flow planes. The pitching moment about the step-keel point is therefore given by the expression

$$M_s = \left[f(\beta)\right]^2\phi_1(A) \frac{\rho\pi}{2} \int_0^{z_s/\tan\tau} (z^2\ddot{z} + 2z\dot{z}^2)(l - s)\, ds$$

or

$$M_s = \frac{\left[f(\beta)\right]^2\phi_1(A)\rho\pi}{6 \tan^2\tau} \left(\frac{\ddot{z}z_s^4}{4} + \dot{z}^2 z_s^3\right) \tag{12}$$

where the pitching moment is taken as positive in the direction of increasing trim.

The pitching moment may be related to the motion of the seaplane measured relative to the water surface by introducing the following expressions from reference 2:

$$z_s = \frac{y}{\cos \tau} \tag{13}$$

$$\dot{z} = \frac{\dot{y}}{\cos \tau} + K \tag{14}$$

where

$$K = (\dot{x}_o - \dot{y}_o \tan \tau) \sin \tau$$

and

$$\ddot{z} = \frac{\ddot{y}}{\cos \tau} \tag{15}$$

Substituting equations (13), (14), and (15) into equation (12) gives

$$M_s = \frac{\left[f(\beta)\right]^2 \phi_1(A) \rho \pi}{6 \sin^2 \tau \cos^3 \tau} \left[\frac{\ddot{y} y^4}{4} + (\dot{y} + K \cos \tau)^2 y^3\right] \tag{16}$$

Equation (16) may be reduced to dimensionless form by introduction of the nondimensional variables defined by equations (5), (6), (7), (8), and (9). Thus, the equation

$$C_{m_s} = C_d^3 \left[\left(\frac{\dot{y}}{\dot{y}_o} + \kappa\right)^2 - \frac{C_l C_d}{4}\right] \tag{17}$$

gives the relationship between the pitching-moment coefficient at any instant and the corresponding draft coefficient, vertical-velocity ratio, and load-factor coefficient, where the pitching-moment coefficient for the step-keel point is defined by

$$C_{m_s} = \frac{M_s}{\dot{y}_o^2} \left(\frac{g}{W}\right) \frac{\phi(A)}{\phi_1(A)} \sin \tau \cos \tau \tag{18}$$

Equations (14), (16), and (18) of reference 2 provide the following relationships which define the motion of the seaplane during the impact:

$$C_l = \frac{3C_d^2\left(\frac{\dot{y}}{\dot{y}_o} + \kappa\right)^2}{1 + C_d^3} \tag{19}$$

$$C_d = \left[\frac{1 + \kappa}{\frac{\dot{y}}{\dot{y}_o} + \kappa} e^{\kappa\left(\frac{1}{1+\kappa} - \frac{1}{\frac{\dot{y}}{\dot{y}_o}+\kappa}\right)} - 1\right]^{1/3} \tag{20}$$

$$C_l = 3\left(\frac{\dot{y}}{\dot{y}_o} + \kappa\right)^2 \cdot \left\{\frac{\frac{\dot{y}}{\dot{y}_o} + \kappa}{1 + \kappa} e^{\kappa\left(\frac{1}{\frac{\dot{y}}{\dot{y}_o}+\kappa} - \frac{1}{1+\kappa}\right)} \left[1 - \frac{\frac{\dot{y}}{\dot{y}_o} + \kappa}{1 + \kappa} e^{\kappa\left(\frac{1}{\frac{\dot{y}}{\dot{y}_o}+\kappa} - \frac{1}{1+\kappa}\right)}\right]^2\right\}^{1/3} \tag{21}$$

Combining equations (17), (19), and (20) results in the following equations:

$$C_{m_s} = \frac{C_d C_l}{3}\left(1 + \frac{C_d^3}{4}\right) \tag{22}$$

$$C_{m_s} = C_d{}^3\left(\frac{\dot{y}}{\dot{y}_o} + \kappa\right)^2 \left[1 - \frac{3}{4}\frac{C_d{}^3}{\left(1 + C_d{}^3\right)}\right] \tag{23}$$

and

$$C_{m_s} = \frac{C_l}{12}\left[\frac{1 + \kappa}{\frac{\dot{y}}{\dot{y}_o} + \kappa} e^{\kappa\left(\frac{1}{1+\kappa} - \frac{1}{\frac{\dot{y}}{\dot{y}_o}+\kappa}\right)} - 1\right]^{1/3} \left[3 + \frac{1 + \kappa}{\frac{\dot{y}}{\dot{y}_o} + \kappa} e^{\kappa\left(\frac{1}{1+\kappa} - \frac{1}{\frac{\dot{y}}{\dot{y}_o}+\kappa}\right)}\right] \tag{24}$$

Applying equations (20) and (21) provides the relationship between the pitching-moment coefficient and the vertical-velocity ratio:

$$C_{m_s} = \frac{\left(\frac{\dot{y}}{\dot{y}_o} + \kappa\right)^2}{4}\left[2 - 3\frac{\frac{\dot{y}}{\dot{y}_o} + \kappa}{1 + \kappa} e^{\kappa\left(\frac{1}{\frac{\dot{y}}{\dot{y}_o}+\kappa} - \frac{1}{1+\kappa}\right)} + \frac{1 + \kappa}{\frac{\dot{y}}{\dot{y}_o} + \kappa} e^{\kappa\left(\frac{1}{1+\kappa} - \frac{1}{\frac{\dot{y}}{\dot{y}_o}+\kappa}\right)}\right] \tag{25}$$

The preceding equations apply at all instants during an impact.

Center of Pressure

The center-of-pressure distance p from the step is defined by

$$p = \frac{M_s}{F_T} \tag{26}$$

From equations (5) and (18), since

$$F_T = -\frac{W}{g}\frac{\ddot{y}}{\cos\tau}$$

$$= \frac{Wn_{i_W}}{\cos\tau}$$

$$= \frac{C_l\dot{y}_o^{\,2}}{\cos\tau}\left(\frac{W}{g}\right)\left(\frac{g}{W}\left\{\frac{[f(\beta)]^2\phi(A)\rho\pi}{6\sin\tau\cos^2\tau}\right\}\right)^{1/3}$$

and

$$M_s = \frac{C_{m_s}\dot{y}_o^{\,2}}{\sin\tau\cos\tau}\left(\frac{W}{g}\right)\frac{\phi_1(A)}{\phi(A)}$$

the relationship that exists at any instant between the dimensionless center-of-pressure coefficient C_{cp} and the moment and load-factor coefficients is given by

$$C_{cp} = \frac{C_{m_s}}{C_l} \tag{27}$$

where

$$C_{cp} = p\sin\tau\,\frac{\phi(A)}{\phi_1(A)}\left(\frac{g}{W}\left\{\frac{[f(\beta)]^2\phi(A)\rho\pi}{6\sin\tau\cos^2\tau}\right\}\right)^{1/3} \tag{28}$$

The combination of equation (22) with (27) gives the relationship between the center-of-pressure coefficient and the draft coefficient:

$$C_{cp} = \frac{C_d}{3}\left(1 + \frac{C_d^{\,3}}{4}\right) \tag{29}$$

Combining equations (24) and (27) gives the following relationship between the center-of-pressure coefficient and the vertical-velocity ratio:

$$C_{cp} = \frac{1}{12}\left[\frac{1+\kappa}{\frac{\dot{y}}{\dot{y}_o}+\kappa}\, e^{\kappa\left(\frac{1}{1+\kappa}-\frac{1}{\frac{\dot{y}}{\dot{y}_o}+\kappa}\right)} - 1\right]^{1/3}\left[3 + \frac{1+\kappa}{\frac{\dot{y}}{\dot{y}_o}+\kappa}\, e^{\kappa\left(\frac{1}{1+\kappa}-\frac{1}{\frac{\dot{y}}{\dot{y}_o}+\kappa}\right)}\right] \tag{30}$$

Substituting the geometric relationship $l = \frac{y}{\sin \tau}$ (see fig. 2) and the definition of the draft coefficient, equation (6), into equations (27) and (28) gives the following expression for the ratio of the center-of-pressure distance to the wetted length:

$$C_r = \frac{C_{m_s}}{C_l C_d} \tag{31}$$

where

$$C_r = \frac{p}{l}\,\frac{\phi(A)}{\phi_1(A)}$$

Combining equation (31) with (20), (21), and (25) provides the relationship between the ratio of the center-of-pressure distance to the wetted length and the vertical-velocity ratio which exists at all instants during the impact:

$$C_r = \frac{1}{4} + \frac{1}{12}\,\frac{1+\kappa}{\frac{\dot{y}}{\dot{y}_o}+\kappa}\, e^{\kappa\left(\frac{1}{1+\kappa}-\frac{1}{\frac{\dot{y}}{\dot{y}_o}+\kappa}\right)} \tag{32}$$

Combining equations (20) and (32) gives the relationship between the ratio of the center-of-pressure distance to the wetted length and the draft coefficient which applies for all values of κ:

$$C_r = \frac{1}{3} + \frac{1}{12} C_d{}^3 \tag{33}$$

Transfer of Moments

The determination of the pitching moment and the center of pressure permits the ready calculation of the hydrodynamic moment about any point on the seaplane. For any point o located at a distance a forward of the step (see fig. 1)

$$M_{o_h} = F_T(p - a)$$

Introducing equation (26) gives

$$M_{o_h} = M_s\left(1 - \frac{a}{p}\right) \tag{34}$$

By use of equations (18) and (28), equation (34) may be written

$$C_{m_{o_h}} = C_{m_s}\left(1 - \frac{a}{p}\right) \tag{35}$$

or

$$C_{m_{o_h}} = \frac{C_{m_s}}{C_{cp}}\left[C_{cp} - a \sin \tau \frac{\phi(A)}{\phi_1(A)}\left(\frac{g}{W}\left\{\frac{[f(\beta)]^2\phi(A)\rho\pi}{6 \sin \tau \cos^2\tau}\right\}\right)^{1/3}\right] \tag{36}$$

where

$$C_{m_{o_h}} = \frac{M_{o_h}}{\dot{y}_o{}^2}\left(\frac{g}{W}\right)\frac{\phi(A)}{\phi_1(A)} \sin \tau \cos \tau \tag{37}$$

Special Conditions

Conditions at maximum moment.– Equation (25) provides the general relationship between the pitching-moment coefficient and the vertical-velocity ratio which applies at all times during an impact. The conditions which exist at the instant when the maximum moment is reached are determined by differentiating equation (25) and setting $\frac{dC_{m_s}}{dt} = 0$. Thus, the equation

$$\frac{1 + \kappa}{\frac{\dot{y}}{\dot{y}_o} + \kappa} e^{\kappa\left(\frac{1}{1+\kappa} - \frac{1}{\frac{\dot{y}}{\dot{y}_o}+\kappa}\right)} + \frac{2\left(\frac{\dot{y}}{\dot{y}_o} + \kappa\right) - \sqrt{13\left(\frac{\dot{y}}{\dot{y}_o}\right)^2 + 32\kappa\frac{\dot{y}}{\dot{y}_o} + 16\kappa^2}}{\frac{\dot{y}}{\dot{y}_o} + 2\kappa} = 0 \qquad (38)$$

provides the relationship between the vertical-velocity ratio at the instant of maximum moment and the approach parameter κ. The substitution of values of $\frac{\dot{y}}{\dot{y}_o}$ obtained by solution of equation (38) into equations (24), (30), (20), and (21) permits the determination of the maximum pitching-moment and center-of-pressure coefficients as well as the draft and load-factor coefficients at the instant of maximum moment. The time coefficient corresponding to the occurrence of maximum moment may be calculated from the variation of C_t with $\frac{\dot{y}}{\dot{y}_o}$ determined in reference 2.

Conditions at maximum acceleration.– The relationship between the vertical-velocity ratio at the instant of maximum acceleration and the approach parameter κ is given by equation (27) of reference 2:

$$\kappa\left[\frac{1}{1 + \kappa} - \frac{1}{\frac{\dot{y}}{\dot{y}_o} + \kappa}\right] - \log_e \frac{\left(9\frac{\dot{y}}{\dot{y}_o} + 6\kappa\right)\left(\frac{\dot{y}}{\dot{y}_o} + \kappa\right)}{\left(7\frac{\dot{y}}{\dot{y}_o} + 6\kappa\right)(1 + \kappa)} = 0 \qquad (39)$$

The vertical-velocity ratio at the instant of maximum acceleration may be determined from the solution of equation (39), and the maximum load-factor coefficient and the draft coefficient at maximum acceleration (reference 2) may be calculated by means of equations (21) and (20).

By use of these values of the vertical-velocity ratio, the pitching-moment and center-of-pressure coefficients at the instant of maximum acceleration may be calculated from equations (25) and (30).

Conditions at maximum draft.- At the instant of maximum draft $\frac{\dot{y}}{\dot{y}_o} = 0$. With this substitution equations (20) and (21) permit the determination of the maximum draft and of the load-factor coefficient corresponding to this instant (reference 2). Similarly the application of equations (25) and (30) provides the following explicit relationships between the pitching-moment and center-of-pressure coefficients at the instant of maximum draft and the approach parameter κ:

$$C_{m_s} = \frac{\kappa^2}{4}\left(2 - 3\,\frac{\kappa}{1+\kappa}\,e^{\frac{1}{1+\kappa}} + \frac{1+\kappa}{\kappa}\,e^{-\frac{1}{1+\kappa}}\right) \tag{40}$$

and

$$C_{cp} = \frac{1}{12}\left(\frac{1+\kappa}{\kappa}\,e^{-\frac{1}{1+\kappa}} - 1\right)^{1/3}\left(\frac{1+\kappa}{\kappa}\,e^{-\frac{1}{1+\kappa}} + 3\right) \tag{40a}$$

The expression relating κ and the ratio of the center-of-pressure distance to the wetted length at the instant of maximum draft is obtained from equation (32):

$$C_r = \frac{1}{4} + \frac{1}{12}\,\frac{1+\kappa}{\kappa}\,e^{-\frac{1}{1+\kappa}} \tag{41}$$

Limiting conditions.- Since the approach parameter κ may range between 0 and ∞, it is desirable to determine the limiting values between which the coefficients of motion at different stages of the impact may vary. The condition of $\kappa = 0$ is obtained when the flight path at contact is normal to the keel of the seaplane. For this condition equations (19) and (20) become

$$C_l = \frac{3C_d^2\left(\frac{\dot{y}}{\dot{y}_o}\right)^2}{1 + C_d^3} \tag{42}$$

and

$$C_d{}^3 = \frac{1 - \frac{\dot{y}}{\dot{y}_o}}{\frac{\dot{y}}{\dot{y}_o}} \tag{43}$$

Combining equations (42) and (43) gives

$$C_l = 3\left(\frac{\dot{y}}{\dot{y}_o}\right)^{7/3}\left(1 - \frac{\dot{y}}{\dot{y}_o}\right)^{2/3} \tag{44}$$

and

$$C_l = \frac{3C_d{}^2}{\left(1 + C_d{}^3\right)^3} \tag{45}$$

The time coefficient may be directly obtained by integrating equation (43):

$$C_t = C_d\left(1 + \frac{1}{4}C_d{}^3\right) \tag{46}$$

or

$$C_t = \left(\frac{1 - \frac{\dot{y}}{\dot{y}_o}}{\frac{\dot{y}}{\dot{y}_o}}\right)^{1/3}\left(1 + \frac{1}{4}\,\frac{1 - \frac{\dot{y}}{\dot{y}_o}}{\frac{\dot{y}}{\dot{y}_o}}\right) \tag{47}$$

For the case where $\kappa = 0$, equation (25) becomes

$$C_{m_s} = \frac{1}{4}\left(\frac{\dot{y}}{\dot{y}_o}\right)\left(\frac{3\dot{y}}{\dot{y}_o} + 1\right)\left(1 - \frac{\dot{y}}{\dot{y}_o}\right) \tag{48}$$

Combining equations (43) and (48) gives

$$C_{m_s} = \frac{C_d{}^3\left(4 + C_d{}^3\right)}{4\left(1 + C_d{}^3\right)^3} \tag{49}$$

For this condition equation (30) gives

$$C_{cp} = \frac{\left(1 - \frac{\dot{y}}{\dot{y}_o}\right)^{1/3}\left(3\,\frac{\dot{y}}{\dot{y}_o} + 1\right)}{12\left(\frac{\dot{y}}{\dot{y}_o}\right)^{4/3}} \tag{50}$$

The relationship between the center-of-pressure coefficient and the draft coefficient is given by equation (29) which is valid for all values of κ.

For $\kappa = 0$ the variation of the ratio of the center-of-pressure distance to the wetted length is obtained from equation (32)

$$C_r = \frac{1}{4} + \frac{1}{12\,\frac{\dot{y}}{\dot{y}_o}} \tag{51}$$

The preceding equations apply at all instants during an impact in which the resultant velocity is normal to the keel and permit the determination of the conditions at specific stages of the impact which may be of interest. For $\kappa = 0$, equation (38) permits the calculation of the vertical-velocity ratio corresponding to the occurrence of maximum moment:

$$\frac{\dot{y}}{\dot{y}_o} = \frac{1}{\sqrt{13} - 2} = 0.6228 \tag{52}$$

The draft coefficient at this instant is determined from equation (43):

$$C_d = \left(\sqrt{13} - 3\right)^{1/3} = 0.8460 \tag{53}$$

while the load-factor coefficient is obtained from equation (44):

$$C_l = \frac{3\left(\sqrt{13} - 3\right)^{2/3}}{\left(\sqrt{13} - 2\right)^3} = 0.5187 \tag{54}$$

Equation (47) permits the calculation of the value of the time coefficient at which the maximum moment occurs:

$$C_t = \left(\sqrt{13} - 3\right)^{1/3} + \frac{1}{4}\left(\sqrt{13} - 3\right)^{4/3} = 0.9741 \tag{55}$$

The maximum moment coefficient is determined from equation (48):

$$C_{m_s} = \frac{\left(\sqrt{13} + 1\right)\left(\sqrt{13} - 3\right)}{4\left(\sqrt{13} - 2\right)^3} = 0.1685 \tag{56}$$

while equation (50) permits the calculation of the center-of-pressure coefficient for the same instant:

$$C_{cp} = \frac{1}{12}\left(\sqrt{13} - 3\right)^{1/3}\left(\sqrt{13} + 1\right) = 0.3247 \tag{57}$$

The ratio of the center-of-pressure distance to the wetted length is obtained from equation (51):

$$C_r = \frac{\sqrt{13} + 1}{12} = 0.3838 \tag{58}$$

In a similar manner, the solution of equation (39) permits the determination of the conditions at the instant of maximum acceleration. As shown by equations (38) to (41) of reference 2 the state of motion at maximum acceleration for $\kappa = 0$ is defined by the following constants:

$$C_d = \left(\frac{2}{7}\right)^{1/3} = 0.6586 \tag{59}$$

$$\frac{\dot{y}}{\dot{y}_o} = \frac{7}{9} \tag{60}$$

$$C_l = 3\left(\frac{2}{7}\right)^{2/3}\left(\frac{7}{9}\right)^3 = 0.6123 \tag{61}$$

and

$$C_t = \left(\frac{2}{7}\right)^{1/3} + \frac{1}{4}\left(\frac{2}{7}\right)^{4/3} = 0.7057 \tag{62}$$

Equation (60) permits the determination of the moment coefficient at maximum acceleration from equation (48). For $\kappa = 0$

$$C_{m_s} = \frac{1}{4}\,\frac{7}{9}\left(\frac{21}{9} + 1\right)\left(1 - \frac{7}{9}\right) = 0.1440 \tag{63}$$

The center-of-pressure coefficient at this instant is obtained from equation (50):

$$C_{cp} = \frac{\left(1 - \frac{7}{9}\right)^{1/3}\left(\frac{21}{9} + 1\right)}{12\left(\frac{7}{9}\right)^{4/3}} = 0.2352 \tag{64}$$

and the ratio of the center-of-pressure distance to the wetted length from equation (51):

$$C_r = \frac{1}{4} + \frac{9}{84} = 0.3571 \tag{65}$$

When $\kappa = 0$ equation (46) shows that the draft always increases with time. Thus, while the downward velocity of the float grows smaller as the impact progresses, a maximum draft is never reached. As discussed in reference 2, this result is due to the fact that, since the deceleration of the seaplane, for $\kappa = 0$, is in the same direction as the resultant velocity (normal to the keel), the seaplane continues along its original path of motion throughout the impact. Thus, only the flow planes directly beneath the keel are affected by the immersion and absorb all the momentum lost by the seaplane. Consequently, an infinite virtual mass (infinite draft) is required to satisfy the condition of zero vertical velocity of the seaplane. This result is due to the neglect of the buoyant forces which, because of the large drafts attained, are of greatest importance at the very high flight-path angles beyond the range of approach conditions applicable to conventional seaplanes. For values of κ other than zero the foregoing result does not apply since part of the momentum lost by the seaplane is contained in the downwash left behind the step, resulting in the attainment of a finite maximum draft (reference 2).

For small values of κ (steep impacts) the differences between the time coefficients corresponding to the occurrence of maximum acceleration, maximum moment, maximum draft, and the rebound from the water surface are large. As the flight path becomes flatter this difference becomes smaller and approaches zero as the planing condition $(\kappa = \infty)$ is reached. For the planing condition the dimensionless variables approach the following limiting values:

$$\lim_{\kappa \to \infty} C_l = \infty$$

$$\lim_{\kappa \to \infty} \frac{\dot{y}}{\dot{y}_o} = 1$$

$$\lim_{\kappa \to \infty} C_d = 0$$

$$\lim_{\kappa \to \infty} C_t = 0$$

$$\lim_{\kappa \to \infty} C_{m_s} = \infty$$

$$\lim_{\kappa \to \infty} C_{cp} = 0$$

$$\lim_{\kappa \to \infty} C_r = \frac{1}{3}$$

THEORETICAL RESULTS AND DISCUSSION

On the basis of the foregoing analysis the variations during an impact of the dimensionless coefficients representing the pitching moment and center of pressure depend solely on the magnitude of the approach parameter κ. For a given value of κ, therefore, the respective variations of the pitching-moment and center-of-pressure coefficients may each be represented by a single curve regardless of the seaplane properties, attitude, or initial velocity. Consequently a single variation exists between the coefficients corresponding to any given stage of the impact $\left(\text{a given value of } \frac{\dot{y}}{\dot{y}_o}\right)$ and the approach parameter κ. The use of dimensionless variables, by thus taking into account such factors as dead-rise angle, weight, trim angle, and velocity

in accordance with the laws governing the variation of the pitching moment and center of pressure with these quantities, permits reduction of the impact conditions to a common basis defined by the approach parameter.

As shown by the form of the coefficients, for a given value of κ the pitching moment and center of pressure corresponding to a given stage of the impact are related to the primary variables constituting the float properties, attitude, and magnitude of the initial velocity by the following proportionalities:

$$M_s \propto \frac{\dot{y}_o^{\,2}}{\sin \tau \cos \tau}\left(\frac{W}{g}\right)\frac{\phi_1(A)}{\phi(A)}$$

and is independent of the angle of dead rise, and

$$p \propto \left\{\frac{\frac{W}{g}}{\left[f(\beta)\right]^2 \phi(A)\ \rho \tan^2\tau}\right\}^{1/3} \frac{\phi_1(A)}{\phi(A)}$$

As a result of the analysis, figures 4 to 13 show the theoretical variations of the pitching-moment coefficient, center-of-pressure coefficient, and ratio of the center-of-pressure distance to the wetted length obtained during step-landing impacts. The solutions include values of κ which correspond to a wide range of approach conditions extending from impacts in which the resultant velocity is normal to the keel $(\kappa = 0)$ to impacts along very shallow flight paths which begin to approach the planing condition. Figures 14 to 20 show the variations with the approach parameter of the conditions which exist at different stages of the impact. In order to compare the conditions at the instant of maximum pitching moment with those existing at other stages of the immersion, solutions for the state of motion and the time corresponding to the occurrence of maximum acceleration, maximum draft, and at the instant of zero draft during rebound, which were previously presented in reference 2, are shown in figures 17 to 20 by the broken-line curves.

Although the dimensionless curves permit the complete determination of the pitching moments as well as the motion experienced by a seaplane during an impact, some interpretation of the results is desirable. For impacts at different values of κ, since both the pitching-moment coefficient and the time coefficient are based on the initial vertical velocity, the actual time histories of the moment will have the same relative shapes as the dimensionless curves if the vertical velocity is the same for each value of κ. Thus the curves shown in figure 7 may be interpreted

as corresponding to different seaplanes landing with the same sinking speed but with different resultant velocities and thus varying flight-path angles, in which case the maximum moment for the shallow approaches (high resultant velocities and large values of κ) will be greater than that for the steeper flight-path angles and will be attained in a shorter time after contact.

On the other hand, a somewhat different interpretation of the dimensionless curves may be given when a particular seaplane landing over a range of flight-path angles is considered. In this case the resultant velocity is more or less constant while the sinking speed, which depends largely on piloting technique, may be varied to provide a range of flight-path angles. As has been previously shown, the pitching moment at any proportional part of the impact cycle varies as the square of the initial vertical velocity while the corresponding time is inversely proportional to the vertical velocity. If the resultant velocity and the trim angle are held constant, steeper flight paths are associated with the smaller values of κ. Since the increase in vertical velocity more than offsets the reduction in pitching-moment coefficient and the increase in time coefficient with decreasing values of κ, the maximum moment obtained with constant resultant velocity and trim angle will be greater for the steeper approaches than at the low flight-path angles and will be attained in a shorter time after contact. The increase in pitching moment with flight-path angle is illustrated by figure 21 which shows the variation with flight-path angle and trim of a dimensionless pitching-moment coefficient based on the resultant velocity at contact.

With regard to the sequence of events during an impact, figures 14 to 20 show that the maximum moment occurs slightly after the maximum acceleration is reached and precedes the attainment of the maximum draft. The state of motion at the instant of maximum moment is only slightly different from the conditions which exist at the instant of maximum acceleration. As might be reasonably expected, for the same sinking speed, a greater time is required to reach a given stage of the impact at the high flight-path angles than is required for the flatter approach conditions. In a similar manner, the differences in the states of motion and the times corresponding to the various stages of the impact are large for small values of κ (high flight-path angles) and become very small as the planing condition is approached.

Although the pitching moment at any stage of an impact varies with the square of the initial vertical velocity, the location of the center of pressure is independent of the initial velocity and is determined primarily by the wetted length. In fact, as is shown by equation (33), the center-of-pressure distance forward of the step is only slightly greater than one-third the wetted length. The fact that this distance is somewhat greater than one-third the wetted length arises from the quadratic nature of the longitudinal distribution of the negative increment in hydrodynamic load accompanying the deceleration of the virtual mass. (See fig. 2.) When this distribution is added vectorially

to the positive linear load variation caused by the expansion of the virtual mass, the resulting distribution of the total load is not quite linear and the center of pressure is shifted slightly forward of the center-of-pressure location for a linear distribution. The extent of this forward shift of the center of pressure depends, of course, on the relative magnitudes of the quadratic and linear distributions and increases with penetration (see equation (33)). Consequently, the most forward location of the center of pressure, both in an absolute sense and in terms of the wetted length, for any given value of κ will be attained at the instant of maximum draft. For impacts at low values of κ this forward shift of the center of pressure in terms of the wetted length may be quite large as a result of the large drafts and the relative magnitudes of the quadratic and linear distributions obtained at the high flight-path angles. For the planing condition, since there is no acceleration, the total load is linearly distributed along the keel and the center of pressure is located at a distance equal to exactly one-third the wetted keel length forward of the step. As shown by figures 13 and 16, even for the practical range of seaplane impact conditions (values of $\kappa > 0.2$) the shift of the center of pressure forward of the one-third point is relatively small and for practical purposes may be neglected in most cases.

COMPARISON WITH EXPERIMENTAL DATA

The applicability of the theoretical results is illustrated by comparisons with experimental data obtained in the Langley impact basin, under controlled conditions in smooth water, with two float forebodies having angles of dead rise of 30° and 40° at the step. The total weights in the tests ranged between approximately 1200 and 1350 pounds. The detailed test conditions are presented in table I. During the tests wing lift was simulated by the action of a pneumatic cylinder and cam system which was designed to apply a constant upward force to the float equal to the total weight.

The experimental results include measurements of the horizontal and vertical components of velocity as well as time histories of the pitching moment. The moments were measured by means of the strain-gage dynamometer truss schematically illustrated in figure 1 and are referred to the front float attachment point as shown in the figure. The original oscillograph records from a typical test are reproduced, greatly reduced, in figure 22.

Experimental pitching-moment time histories, as derived from the oscillograph records, are shown in figures 23 to 26. These data are compared with theoretical time histories of the total pitching moment about the front attachment point as well as with theoretical time histories of the hydrodynamic pitching moment about this point.

The time histories of the hydrodynamic pitching moment were calculated by application of equations (35) and (37) in conjunction

with the analytical results plotted in figures 7 and 12. The dimension a in equation (35), which represents the distance from the step to the front attachment point, was measured as 2.89 feet for the two floats tested. In converting from dimensionless variables to the dimensional quantities moment and time, it is necessary to introduce values for the functions $f(\beta)$, $\phi(A)$, and $\phi_1(A)$. Equations (10) and (11) present expressions for $f(\beta)$ and $\phi(A)$ which have been shown to be valid for a wide range of dead-rise and trim angles. Since $\phi_1(A)$ has not been evaluated at the present time, it was assumed that the aspect-ratio correction to the total load $\phi(A)$ applies uniformly to all flow planes; that is, $\phi_1(A) = \phi(A)$. From the nature of this approximation it would appear that this assumption does not involve serious errors.

In order to properly compare the theoretical and experimental results, the inertia and static moments, introduced by the fact that the center of gravity of the model did not coincide with the center of moments, must be added to the hydrodynamic moment about the front attachment point. The increment in pitching moment arising from this source is given by the equation

$$\Delta M_o = W_f \left[\frac{\ddot{y}}{g} \frac{b}{\cos \tau} - (b \cos \tau + c \sin \tau)\right] \tag{66}$$

Thus the total pitching moment referred to the point o is expressed by

$$M_{o_T} = \frac{\dot{y}_o^{\,2}}{g \cos \tau} \left[\frac{C_{m_s} W}{\sin \tau} \frac{\phi_1(A)}{\phi(A)} - C_l \left(\frac{g}{W} \left\{\frac{[f(\beta)]^2 \phi(A) \rho \pi}{6 \sin \tau \cos^2 \tau}\right\}\right)^{1/3} (aW + bW_f)\right]$$

$$- W_f(b \cos \tau + c \sin \tau) \tag{67}$$

where the dimensions b and c define the location of the center of gravity relative to the center of moments, as shown in figure 1. Values of b and c for each of the configurations tested are given in table I.

Figures 23(a), (b), and (c) show the results of three tests of the float with 30° angle of dead rise at 12° trim. All three tests were made at approximately the same flight-path angle of about 5° and, therefore, closely correspond to a single value of the approach parameter κ

equal to about 2.2. Two of the tests were made with almost identical resultant velocities. The third test was made at a velocity approximately 60 percent greater than that for the first two runs. The theoretical results were calculated for values of the initial vertical velocity measured in the tests and for a value of $\kappa = 2$, which approximately corresponds to the magnitude of the approach parameter associated with the tests. The theoretical total pitching moments appear to be in substantial agreement with the results measured in the tests.

Figure 24 is a composite plot of the quantity

$$\frac{M_{o_T} + W_f(b \cos \tau + c \sin \tau)}{\frac{W}{g} \dot{y}_o^{\,2}}$$

$$= \left[\frac{C_{m_s}}{\sin \tau} \frac{\phi_1(A)}{\phi(A)} - C_l \left(\frac{g}{W}\left\{\frac{\left[f(\beta)\right]^2 \phi(A) \rho \pi}{6 \sin \tau \cos^2 \tau}\right\}\right)^{1/3} \left(a + b \frac{W_f}{W}\right)\right] \frac{1}{\cos \tau} \qquad (67a)$$

against the variable $t\dot{y}_o$. For the three tests previously discussed, since all parameters except the resultant velocity were held constant, equation (67a) and the form of the time coefficient show that the results of all three tests should be reduced to the single theoretical variation given by the solid-line curve. As is evident from the figure, this result is closely attained. The extent of the deviations which do exist may be taken as a direct indication of the consistency of the experimental data. The oscillatory nature of the results of some of the tests (see fig. 22) is attributed to structural vibrations induced in the equipment by the magnitude of the catapulting accelerations required to produce the relatively high horizontal velocities attained in the tests.

Figures 25 and 26 show comparisons of theoretical and experimental pitching-moment time histories for typical impacts of a float with a 40° angle of dead rise at trim angles of 9° and 6° and values of the approach parameter κ approximately equal to 1. Comparisons between theoretical and experimental maximum total pitching moments for this float are presented in figures 27(a), (b), and (c) for trim angles of 12°, 9°, and 6°. In order to reduce the increment in pitching moment due to the displacement of the center of gravity from the center of moments, another set of tests was made, at 12° trim, with the float weighted to move the center of gravity rearward to a position vertically in line with the front attachment fitting. The results of these tests

are shown in figure 28. As is evident from the figures, the theoretical results appear to be in good agreement with the experimental data. A more exact evaluation of the end-flow correction to the pitching moment $\phi_1(A)$, which in this comparison has been taken equal to the end-flow correction to the total load $\phi(A)$, should result in even better agreement between the calculated and experimental results. In the absence of suitable pressure-distribution data, the favorable results of this comparison may be considered an indirect indication of the validity of the longitudinal distribution of the hydrodynamic load (running load) specified by the theory.

SUMMARY OF RESULTS

Theoretical

The preceding analysis of the pitching moments experienced by V-bottom seaplanes during step-landing impacts has shown that:

1. The pitching moment about the step and the center-of-pressure distance forward of the step may be represented in generalized form by means of the following dimensionless variables: pitching-moment coefficient

$$C_{m_s} = \frac{M_s}{\dot{y}_o^2}\left(\frac{g}{W}\right)\frac{\phi(A)}{\phi_1(A)} \sin \tau \cos \tau$$

and center-of-pressure coefficient

$$C_{cp} = p \sin \tau\left(\frac{g}{W}\left\{\frac{[f(\beta)]^2\phi(A)\rho\pi}{6 \sin \tau \cos^2\tau}\right\}\right)^{1/3}$$

It is also shown that the variation of these dimensionless quantities during an impact is governed solely by the magnitude of the approach parameter

$$\kappa = \frac{\sin \tau}{\sin \gamma_o} \cos (\tau + \gamma_o)$$

which depends only on the trim and the flight path at the instant of initial contact with the water surface. For a given value of κ, therefore, the respective variations of the pitching-moment and center-of-pressure coefficients may each be represented by a single curve regardless of what the seaplane properties, attitude, or initial conditions may be. Consequently a single variation exists between the coefficients existing at any stage of the impact and the approach

parameter κ. The expression of the pitching moment and center of pressure in terms of dimensionless variables, by thus taking into account such factors as angle of dead rise, weight, trim angle, and initial velocity, permits reduction of all impact conditions to a common basis defined by the approach parameter and leads to a simplified presentation of both theoretical and experimental results.

2. From the form of the pitching-moment coefficient it can be seen that the pitching moment about the step at any given stage of the impact is independent of the angle of dead rise.

3. The maximum pitching moment about the step is attained slightly after the maximum acceleration (load) is reached and occurs prior to the attainment of the maximum draft. The state of motion of the seaplane and the time corresponding to the instant of maximum pitching moment are only slightly different from the conditions which exist at the instant of maximum acceleration. The differences in the coefficients representing the pitching moments, the states of motion, and the times corresponding to given stages of the impact $\left(\text{given values of } \frac{\dot{y}}{\dot{y}_o}\right)$, such as the instants of maximum acceleration, maximum pitching moment, maximum draft, or zero draft during rebound, are greatest at the low values of the approach parameter κ (steep flight paths for conventional trim angles) and decrease as the planing condition is approached.

4. For given seaplane properties, attitude, and constant vertical velocity, the pitching moments about the step are greater for the higher values of the approach parameter κ (corresponding to low flight-path angles and high resultant velocities, for conventional trim angles) than those at the lower values of κ (steep flight paths and low resultant velocities, for conventional trim angles) and are attained in a shorter time after contact. For a given resultant velocity, on the other hand, the greater pitching moments are attained at the lower values of κ.

5. In a step impact the center of pressure is located at a distance only slightly greater than one-third the wetted keel length forward of the step. The relationship between the center-of-pressure distance and the wetted length is independent of the magnitude of the initial velocity and is determined primarily by the wetted length. For the planing condition the center of pressure is located at a distance exactly equal to one-third the wetted keel length forward of the step and is shifted slightly forward with decreasing values of the approach parameter κ. The most forward center-of-pressure locations, both in an absolute sense and in terms of the wetted length, are obtained in conjunction with the large draft coefficients reached at the low values of κ (steep flight paths for conventional trim angles). For the practical range of impact conditions $(\kappa \geqq 0.2)$, however, only small errors will be introduced if the resultant force is assumed to act at a distance equal to one-third the wetted keel length forward of the step.

Experimental

Comparison of the theoretical results with test data obtained in the Langley impact basin with floats having angles of dead rise of 30° and 40° at the step indicates that, within the limits of experimental error, the calculated pitching moments are in good agreement with the experimental results.

CONCLUDING REMARKS

A theoretical investigation has been made of the hydrodynamic pitching moments experienced by V-bottom seaplanes during step-landing impacts. The analysis shows that the pitching moment and the center-of-pressure location may be represented in generalized form by means of dimensionless variables, respectively designated the pitching-moment coefficient and the center-of-pressure coefficient, which take into account such factors as the seaplane weight, angle of dead rise, trim angle, and initial velocity. The variation of these coefficients during an impact is governed by the magnitude of the approach parameter κ determined by the trim and the initial flight-path angle.

Equations are presented from which the variation of the pitching-moment and center-of-pressure coefficients have been calculated for a wide range of conditions extending from impacts along shallow flight-path angles approaching planing to very steep impacts in which the resultant velocity is normal to the keel. Solutions are also presented for the conditions which exist at the instants of maximum acceleration, maximum pitching moment, maximum draft, and at the instant of zero draft during rebound.

Comparisons of theoretical pitching-moment time histories and values of the maximum pitching moment with experimental data obtained in the Langley impact basin with floats of 30° and 40° angle of dead rise indicate that the calculated results are in good agreement with the measured values.

Langley Memorial Aeronautical Laboratory
National Advisory Committee for Aeronautics
Langley Field, Va., January 30, 1948

REFERENCES

1. Mayo, Wilbur L.: Analysis and Modification of Theory for Impact of Seaplanes on Water. NACA Rep. No. 810, 1945.

2. Milwitzky, Benjamin: A Generalized Theoretical and Experimental Investigation of the Motions and Hydrodynamic Loads Experienced by V-Bottom Seaplanes during Step-Landing Impacts. NACA TN No. 1516, 1948.

3. Wagner, Herbert: Über Stoss- und Gleitvorgänge an der Oberfläche von Flüssigkeiten. Z.f.a.M.M., Bd. 12, Heft 4, Aug. 1932, pp. 193-215.

4. Pabst, Wilhelm: Theory of the Landing Impact of Seaplanes. NACA TM No. 580, 1930.

5. Miller, Robert W., and Leshnover, Samuel: Hydrodynamic Impact Loads in Smooth Water for a Prismatic Float Having an Angle of Dead Rise of 30°. NACA TN No. 1325, 1947.

TABLE I.- TEST CONDITIONS

[a = 2.89 ft]

τ (deg)	V_{v_o} (ft/sec)	V_{h_o} (ft/sec)	γ_o (deg)	κ	$M_{o_{b_{max}}}$ (lb-ft)
$\beta = 30^\circ$; W = 1231 lb; W_r = 400 lb; b = 0.5 ft; c = 1.5 ft					
12	4.95	54.55	5.18	2.20	-4000
	5.28	57.89	5.21	2.19	-4350
	7.92	87.50	5.17	2.20	-10800
$\beta = 40^\circ$; W = 1213 lb; W_r = 350 lb; b = 1.05 ft; c = 1.81 ft					
12	3.13	90.09	1.99	5.810	-3551
	3.70	90.09	2.35	4.913	-3145
	2.92	68.49	2.44	4.729	-2479
	3.98	90.09	2.53	4.559	-4353
	3.20	67.57	2.71	4.253	-2357
	4.98	90.09	3.16	3.640	-5906
	4.27	68.03	3.59	3.198	-3230
	4.12	55.87	4.22	2.713	-2858
	5.33	68.03	4.48	2.552	-3351
	3.27	40.49	4.62	2.473	-1818
	5.69	68.49	4.75	2.404	-4751
	7.54	89.29	4.83	2.364	-8857
	7.68	90.91	4.83	2.364	-8421
	7.89	90.91	4.96	2.300	-8761
	8.75	91.00	5.49	2.073	-10333
	3.98	39.37	5.77	1.969	-2197
	5.76	56.50	5.82	1.952	-10372
	9.10	89.29	5.82	1.952	-3756
	9.24	90.09	5.86	1.938	-10141
	3.06	29.33	5.96	1.905	-1272
	4.34	40.98	6.05	1.876	-2351
	3.34	30.40	6.27	1.808	-1485
	7.61	68.49	6.34	1.787	-6541
	7.75	68.49	6.46	1.753	-6271
	7.82	68.49	6.51	1.739	-6624
	9.03	68.03	7.56	1.489	-7722
	4.34	30.40	8.12	1.382	-1716
	5.83	40.65	8.16	1.376	-3025
	8.11	56.18	8.21	1.365	-5193
	3.48	23.26	8.51	1.316	-1157
	9.39	56.18	9.49	1.173	-6573
	4.05	22.83	10.06	1.103	-1379
	4.34	22.57	10.88	1.015	-1485
	7.96	40.98	10.99	1.004	-3865
	7.75	39.53	11.09	.994	-3137
	9.24	39.84	13.06	.834	-5039
	9.46	39.84	13.36	.813	-5001
	8.11	30.12	15.07	.712	-3198
	9.10	30.03	16.86	.628	-3865
	9.53	29.67	17.81	.590	-4295
	7.96	23.04	19.06	.545	-2479
	9.46	23.15	22.23	.454	-3448

τ (deg)	V_{v_o} (ft/sec)	V_{h_o} (ft/sec)	γ_o (deg)	κ	$M_{o_{b_{max}}}$ (lb-ft)
$\beta = 40^\circ$; W = 1213 lb; W_r = 350 lb; b = 1.05 ft; c = 1.81 ft (Concluded)					
9	2.92	60.24	2.78	3.157	-2134
	2.98	58.48	2.92	3.005	-2023
	3.12	44.64	4.00	2.185	-1503
	3.27	43.48	4.30	2.030	-1672
	8.60	86.96	5.65	1.537	-6990
	8.67	86.20	5.74	1.513	-8197
	8.60	76.34	6.43	1.347	-5907
	9.03	77.51	6.65	1.301	-3564
	8.89	65.79	7.70	1.118	-3648
	8.75	63.69	7.82	1.101	-5464
	8.60	57.14	8.56	1.002	-5143
	9.10	58.82	8.79	.975	-3372
	8.96	51.55	9.86	.864	-4718
	9.46	46.08	11.60	.728	-3952
	9.24	44.44	11.75	.718	-4620
	9.46	45.45	11.76	.718	-5052
	9.24	35.59	14.55	.571	-3756
6	2.77	43.10	3.68	1.605	-1169
	2.99	43.67	3.92	1.506	-1194
	2.99	43.48	3.93	1.502	-1286
	8.67	85.47	5.79	1.014	-5354
	8.75	65.36	7.63	.765	-4140
	9.03	66.22	7.77	.751	-4552
	8.96	60.97	8.36	.697	-4281
	8.96	58.47	8.46	.688	-4403
	8.75	44.25	11.19	.515	-3421
	8.89	43.29	12.61	.495	-3114
	9.03	43.47	11.74	.489	-3231
	8.89	35.21	14.17	.401	-3190
	8.75	34.60	14.19	.400	-3199
	8.89	34.13	14.60	.388	-3032
$\beta = 40^\circ$; W = 1343 lb; W_r = 590 lb; b = -0.283 ft; c = 1.458 ft					
12	3.37	70.42	2.74	4.206	-2144
	4.16	71.94	3.31	3.473	-2843
	4.24	70.92	3.42	3.360	-2728
	5.96	95.24	3.58	3.208	-5642
	6.17	95.24	3.71	3.093	-6328
	3.30	44.44	4.25	2.694	-1225
	3.30	44.05	4.28	2.674	-1418
	3.59	44.64	4.60	2.484	-1463
	7.90	86.21	5.24	2.174	-6091
	4.16	44.44	5.35	2.128	-1460
	7.04	72.46	5.55	2.050	-4891
	9.26	91.74	5.76	1.972	-8785
	6.32	34.01	10.53	1.051	-1593
	8.19	43.29	10.71	1.032	-3174
	8.11	39.53	11.39	.948	-2905

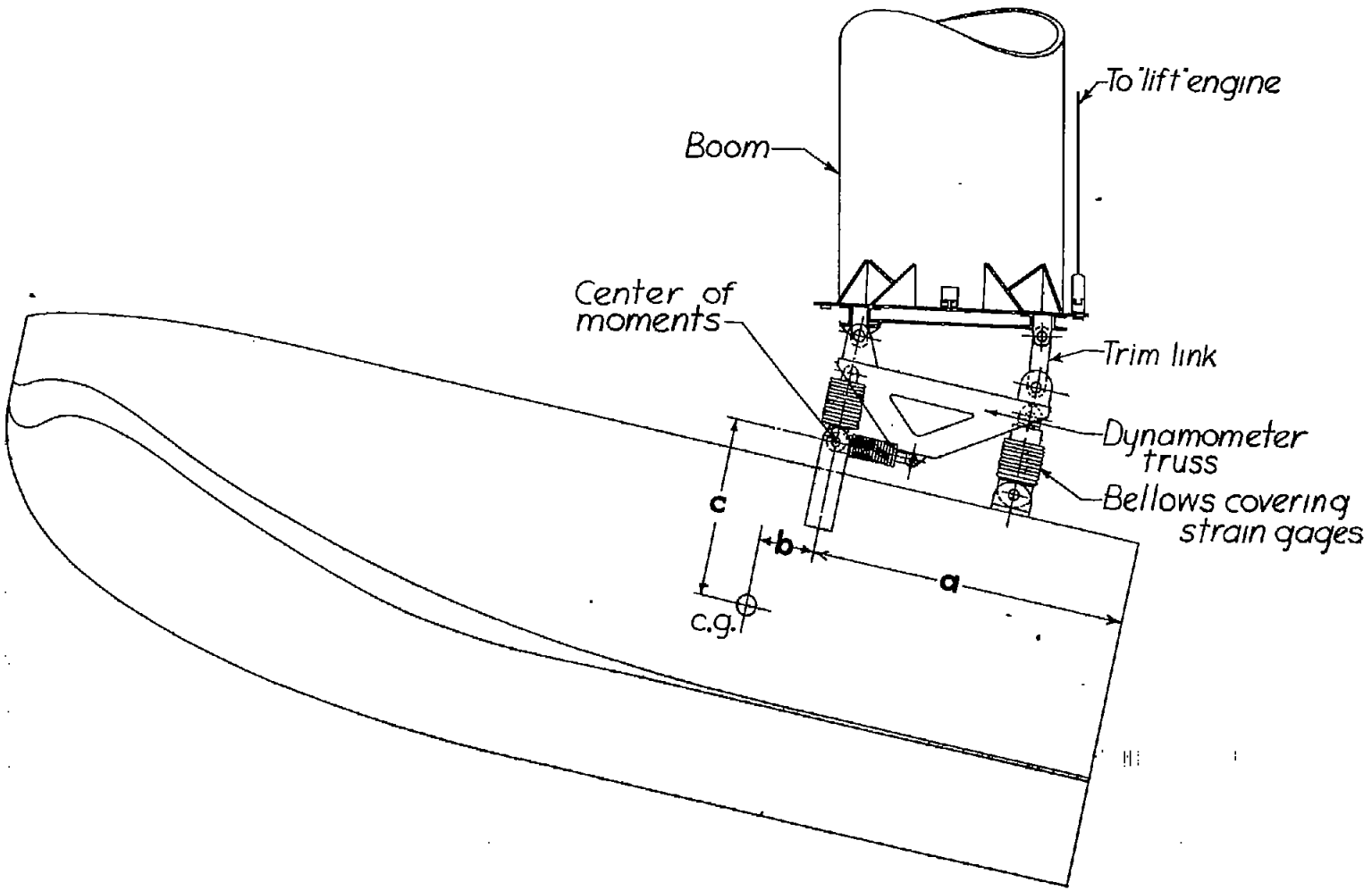

Figure 1.– Float-forebody model attached to boom of impact-basin carriage by means of dynamometer truss.

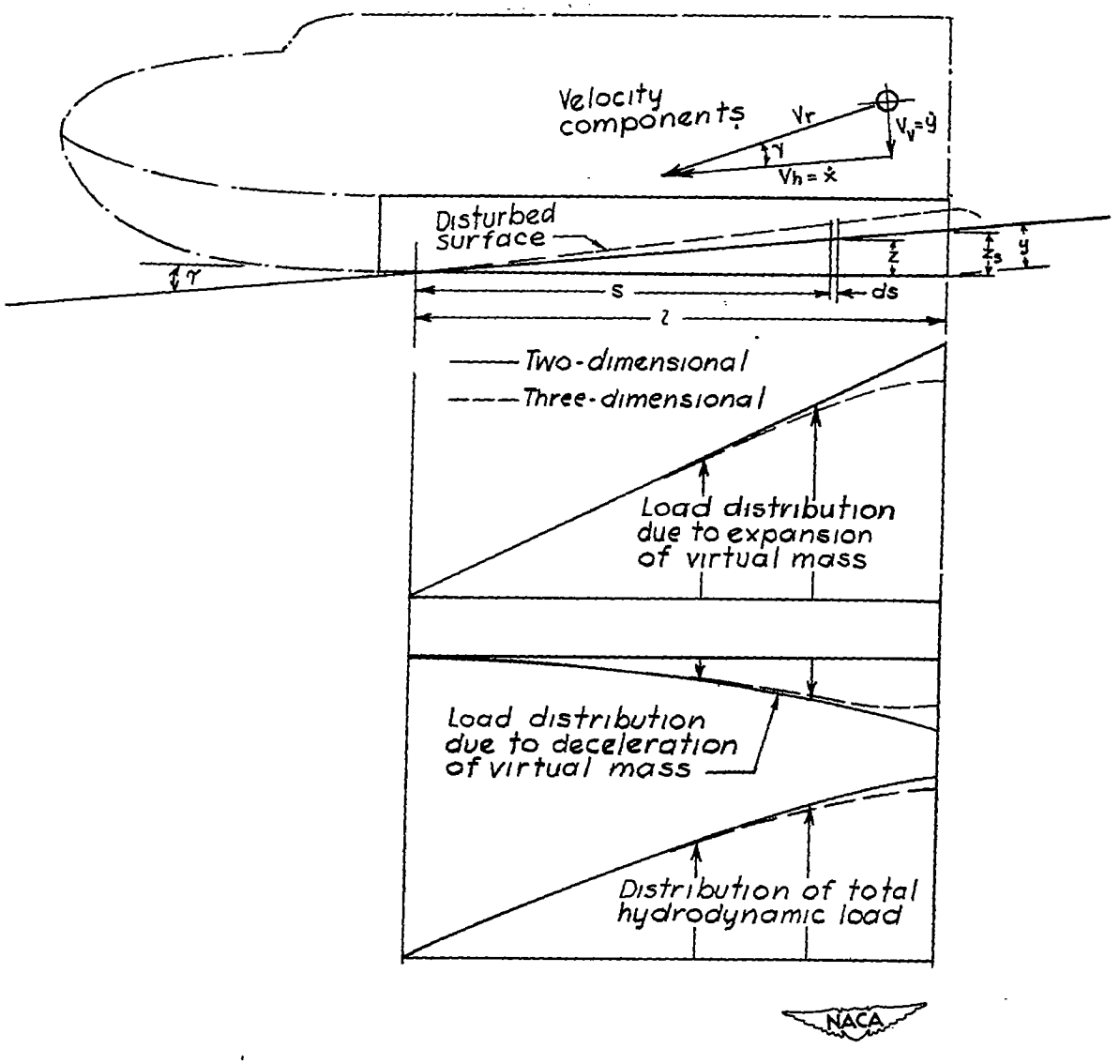

Figure 2. — Schematic representation of the impact of a seaplane with a prismatic bottom.

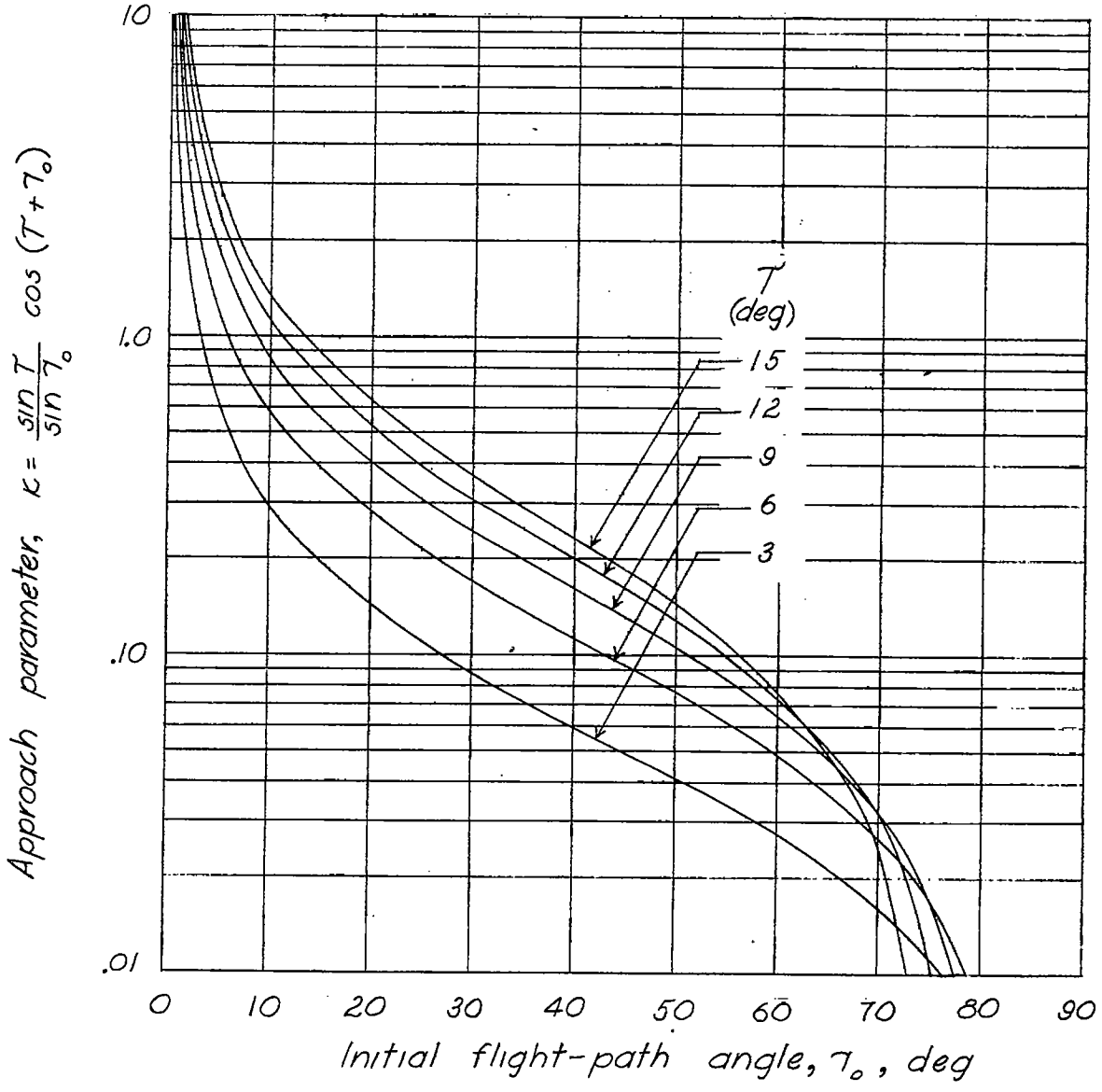

Figure 3. — Variation of approach parameter with trim and flight-path angle.

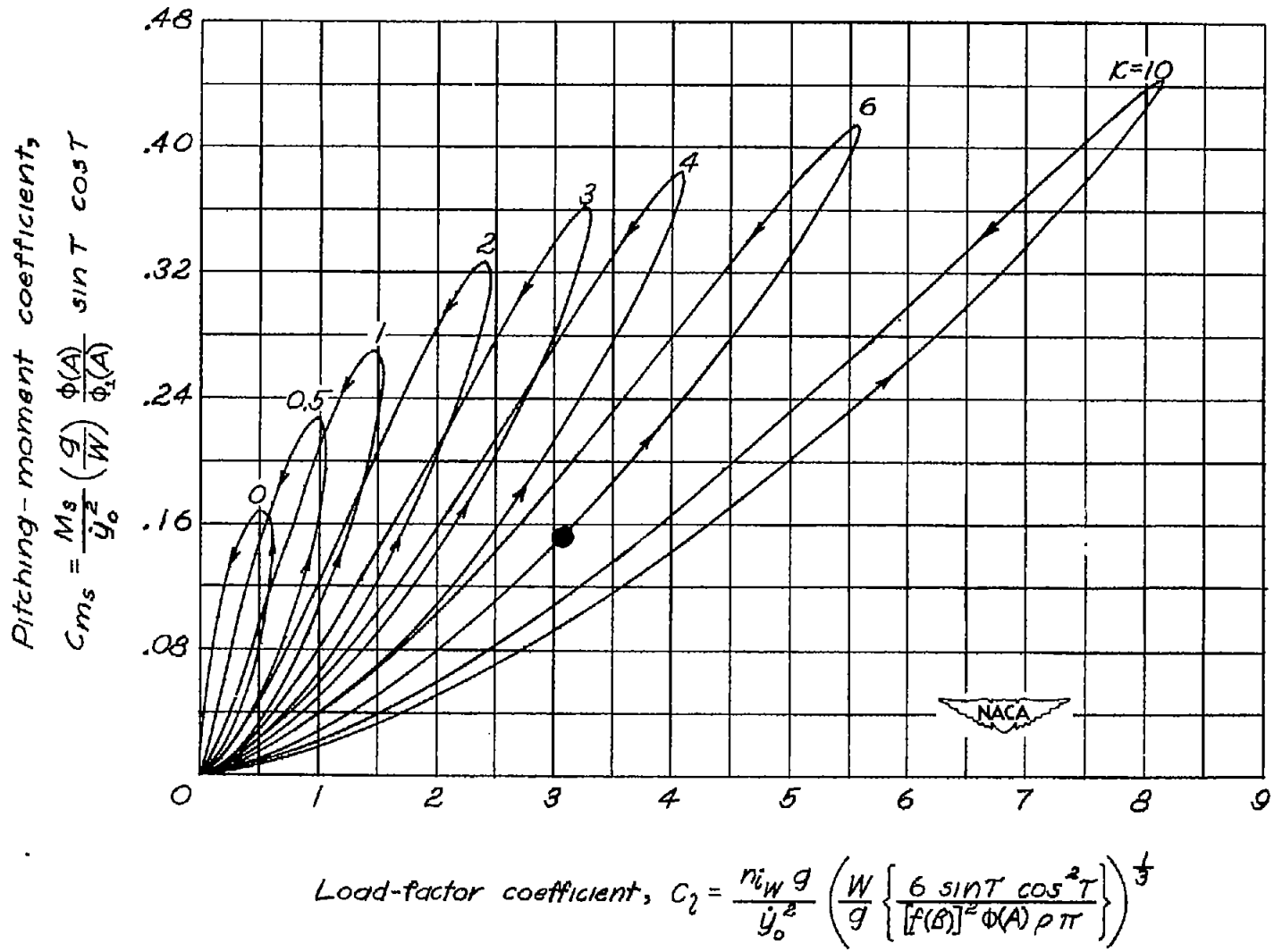

Figure 4.—Theoretical variation of pitching moment with load factor.

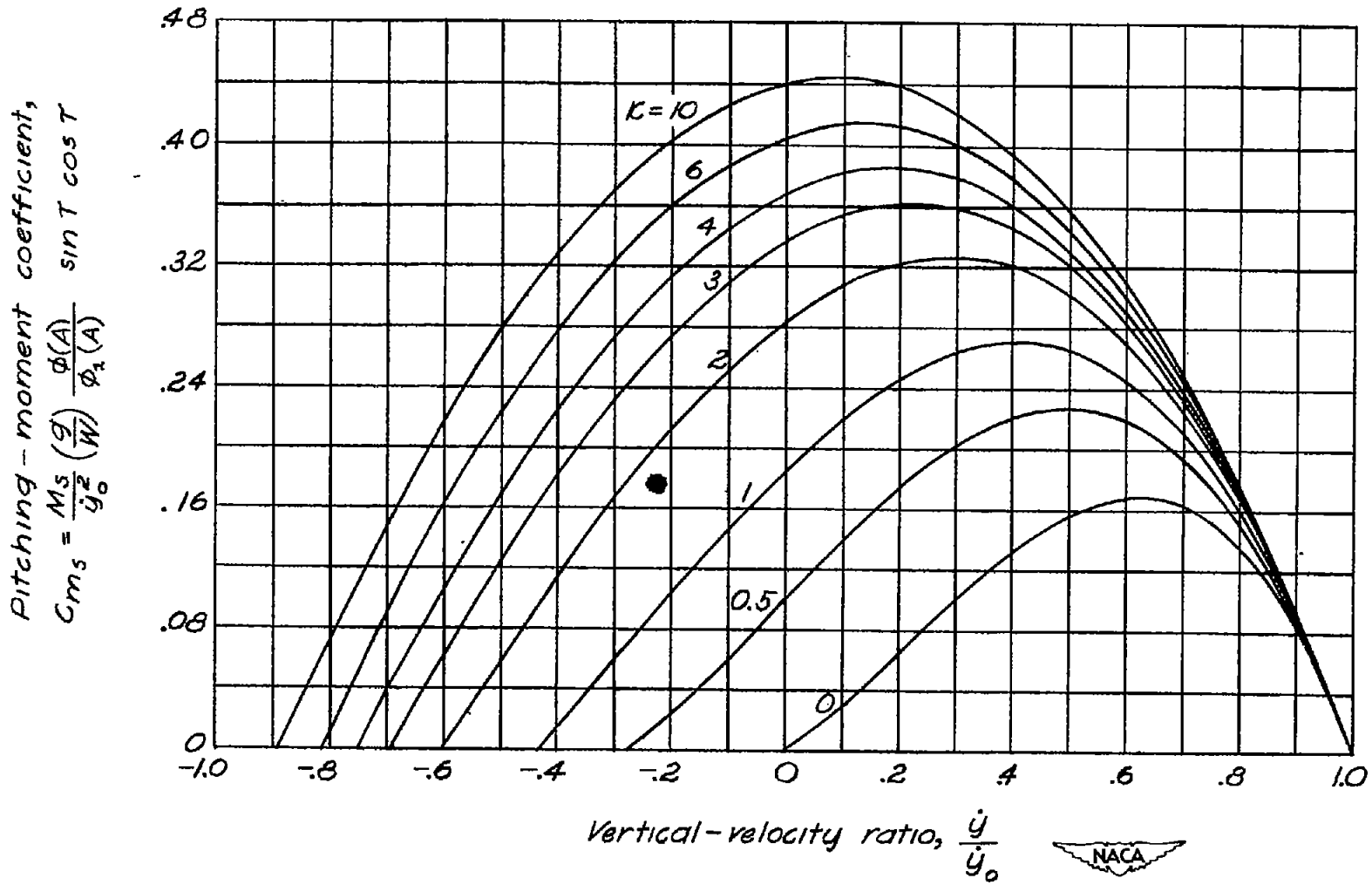

Figure 5.—Theoretical variation of pitching moment with vertical velocity.

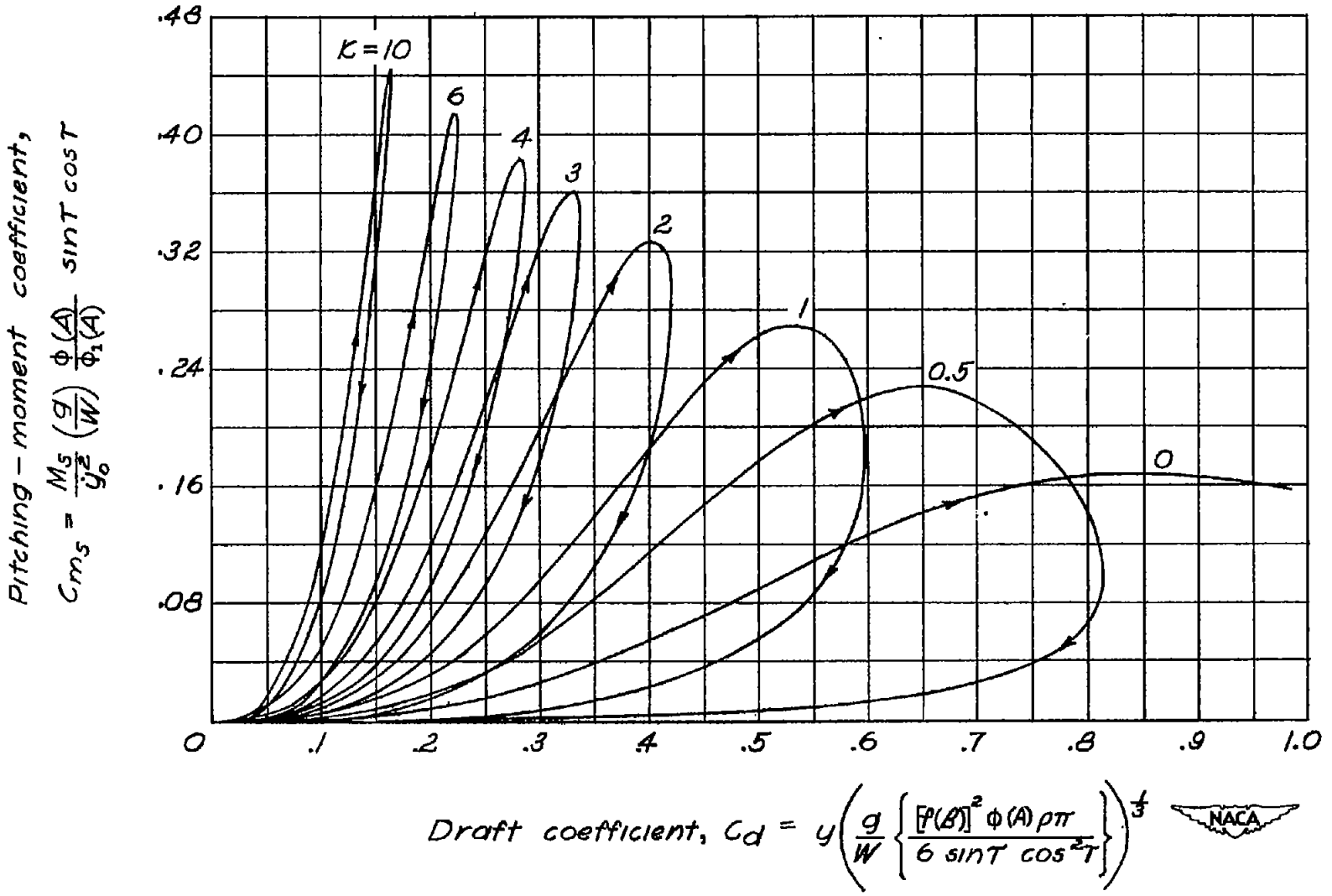

Figure 6.— Theoretical variation of pitching moment with draft.

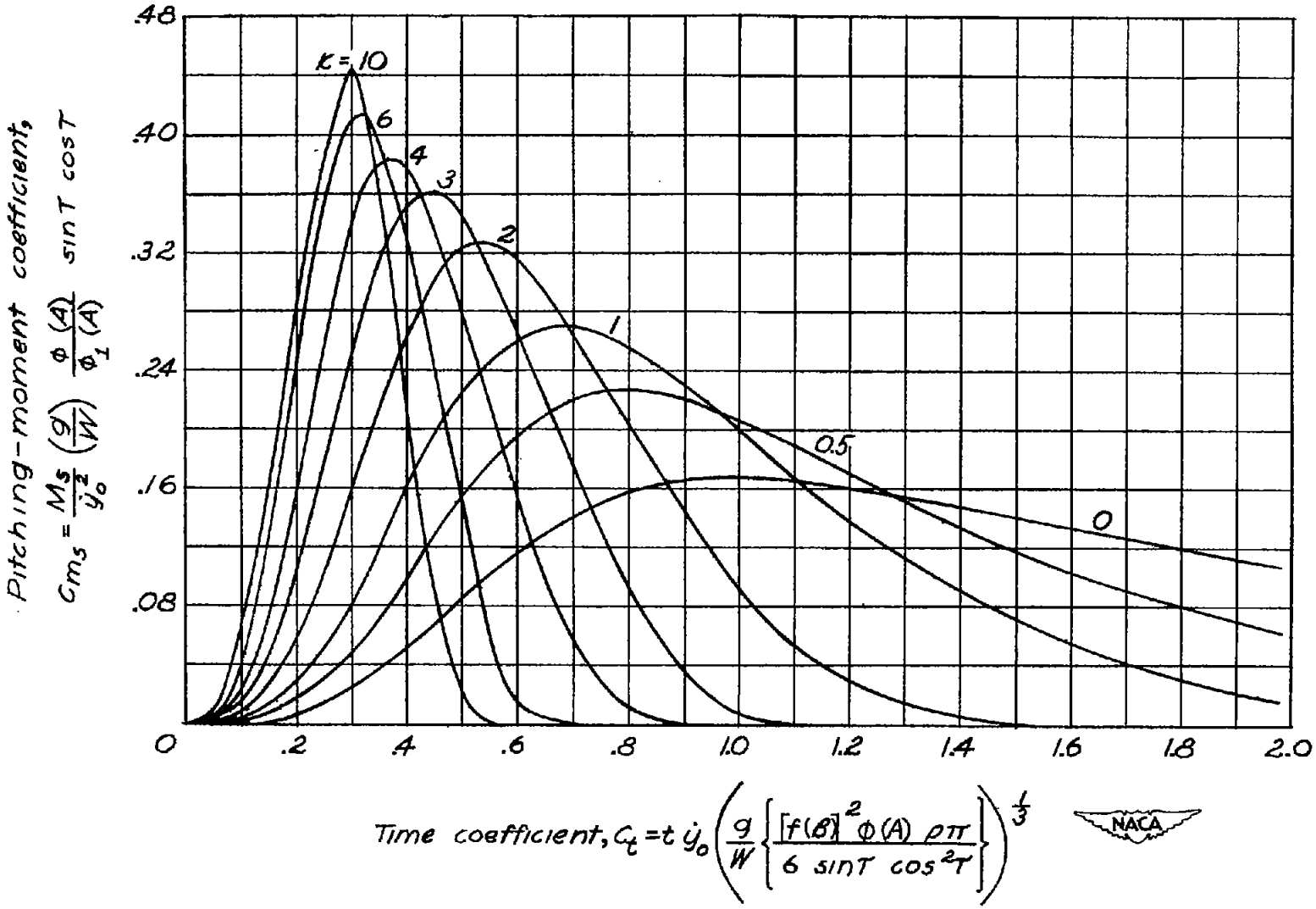

Figure 7.— Theoretical variation of pitching moment with time.

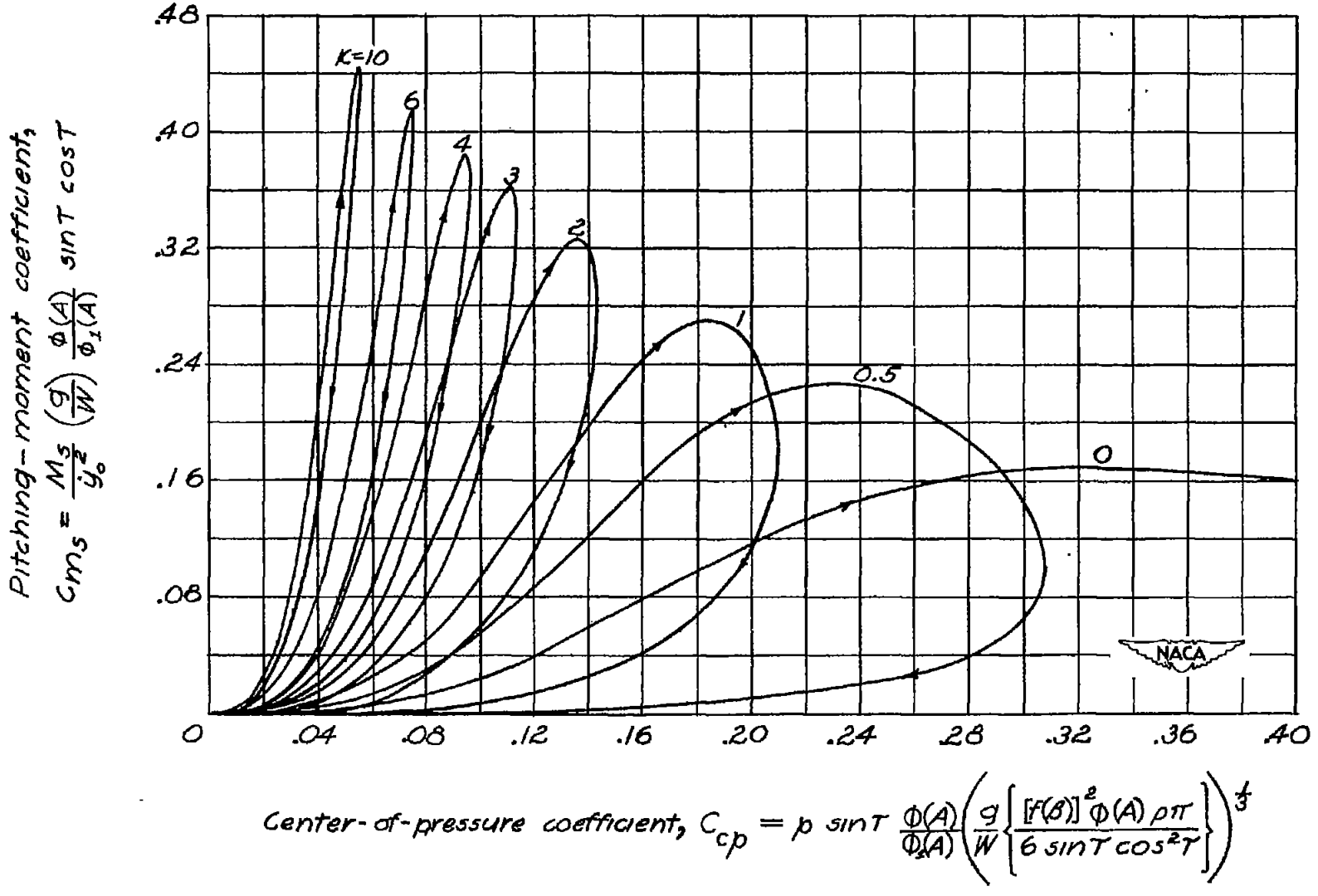

Figure 8.—Theoretical variation of pitching moment with center of pressure.

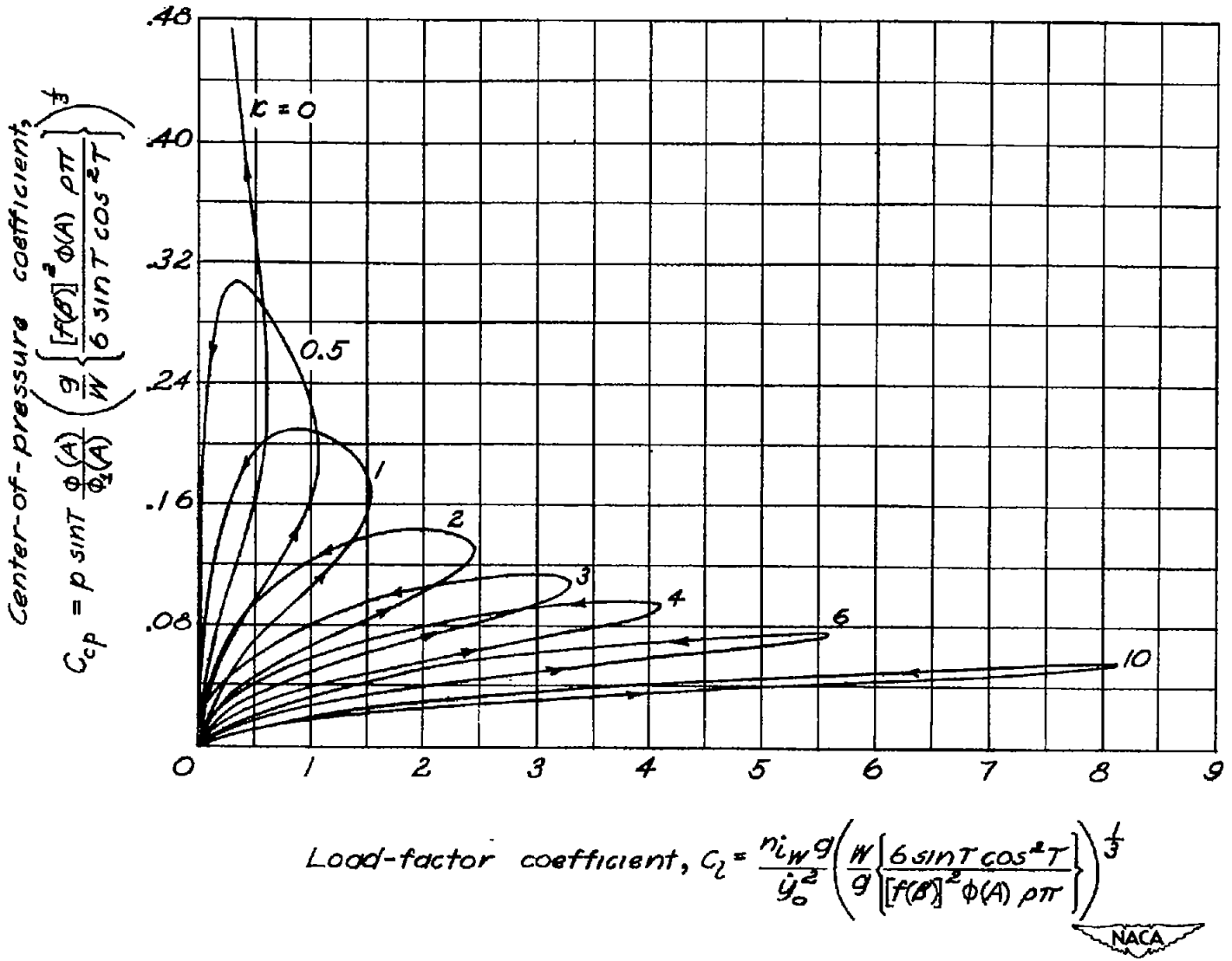

Figure 9.—Theoretical variation of center of pressure with load factor.

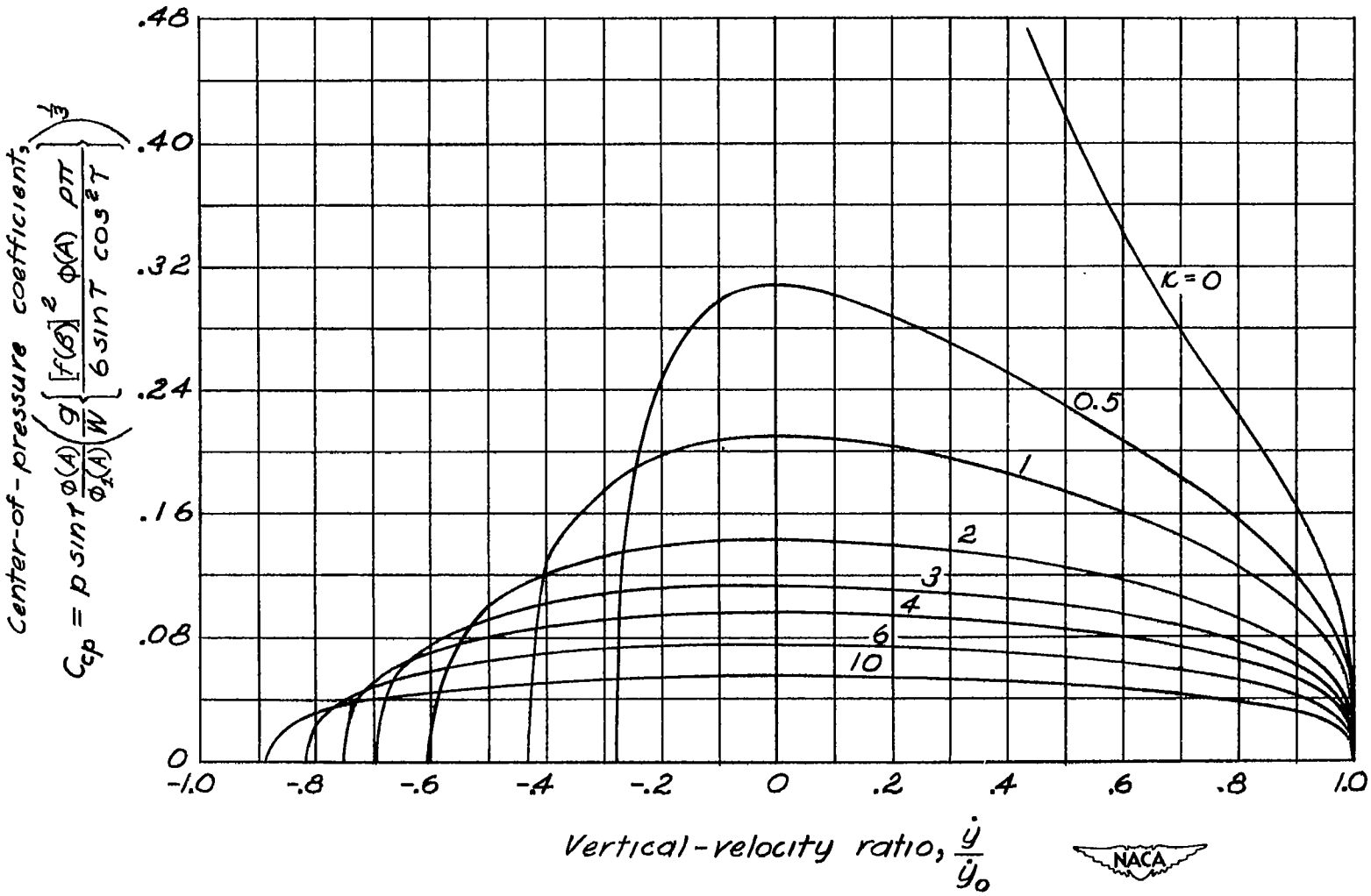

Figure 10. — Theoretical variation of center of pressure with vertical velocity.

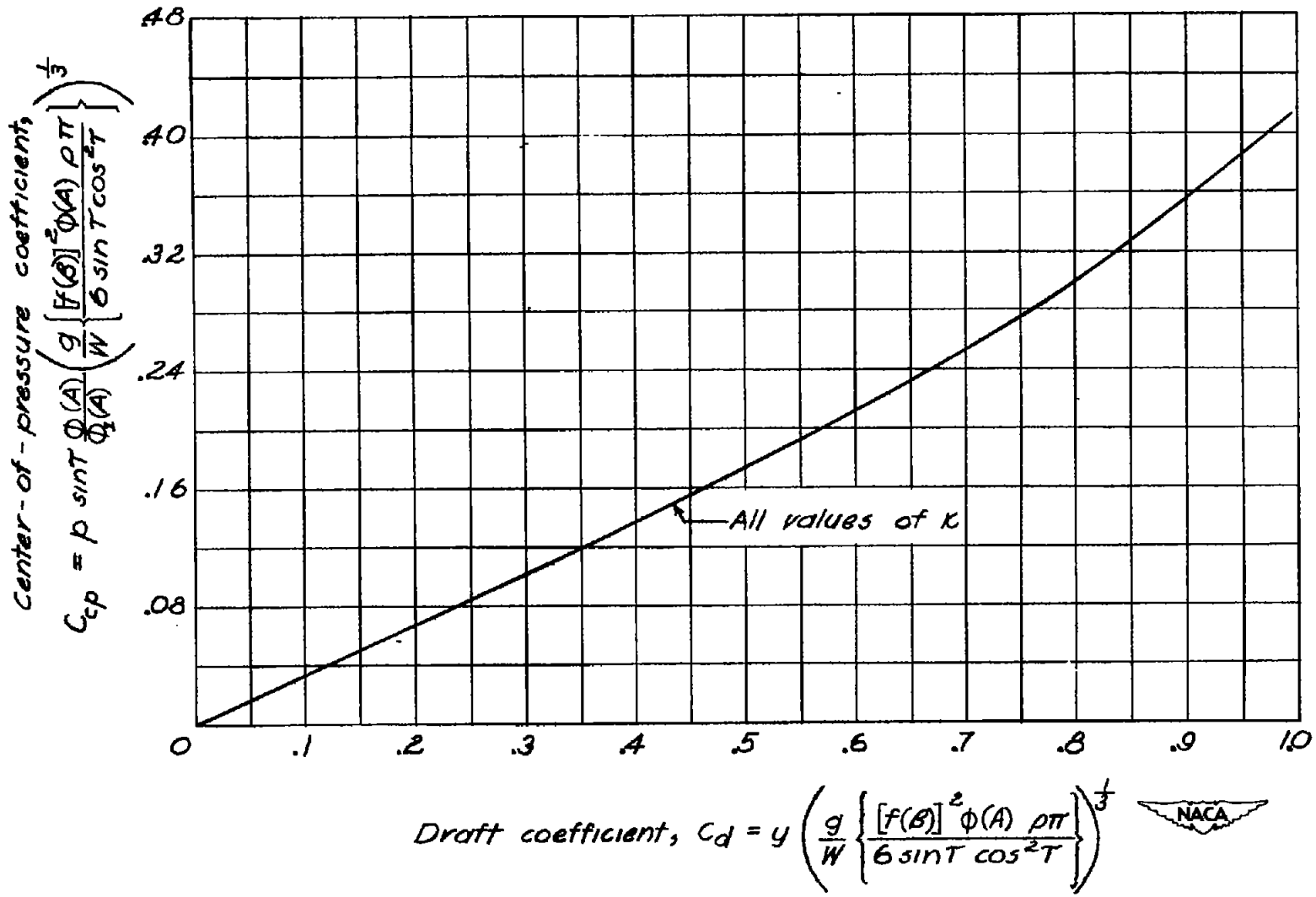

Figure 11.—Theoretical variation of center of pressure with draft.

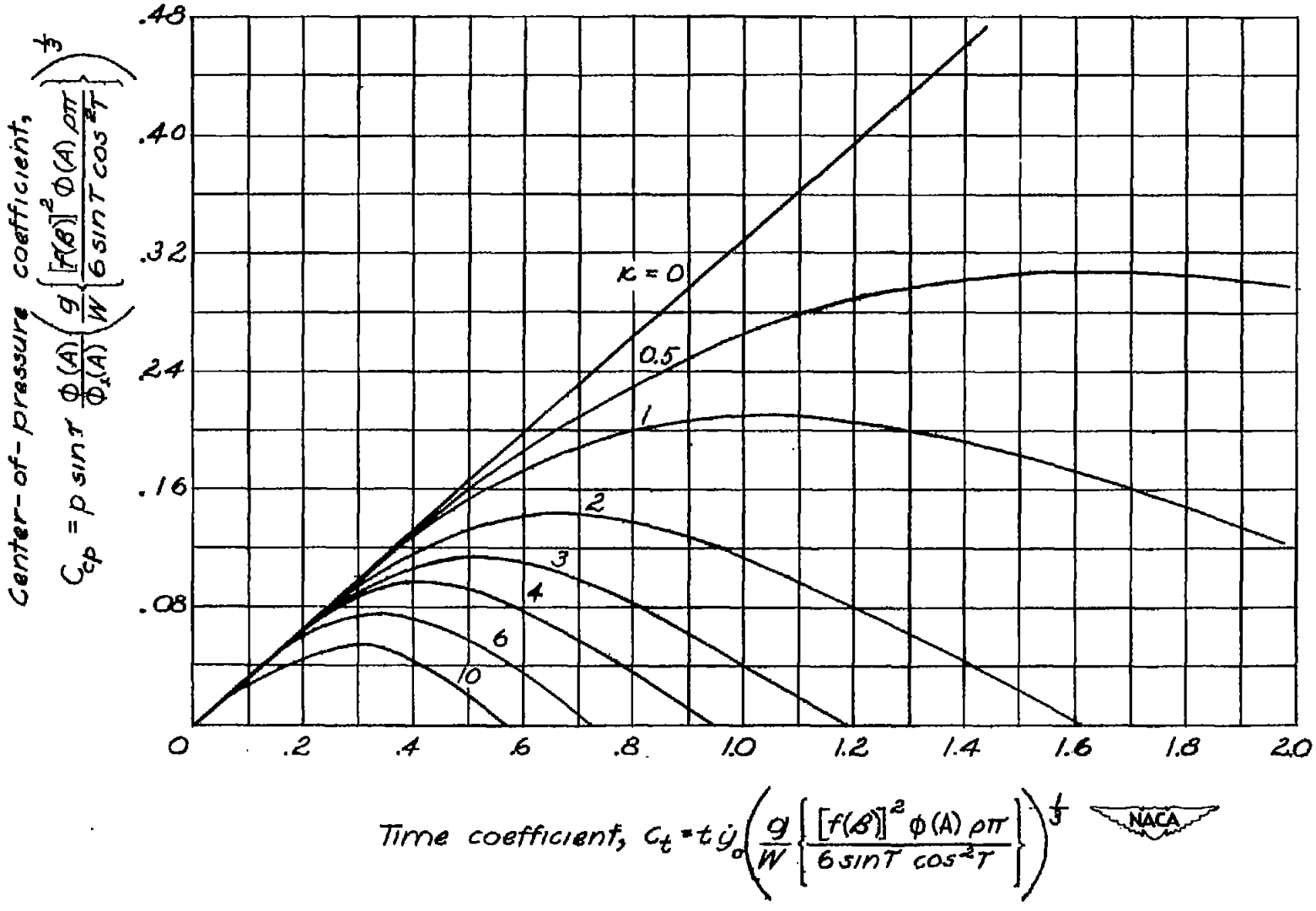

Figure 12.— Theoretical variation of center of pressure with time.

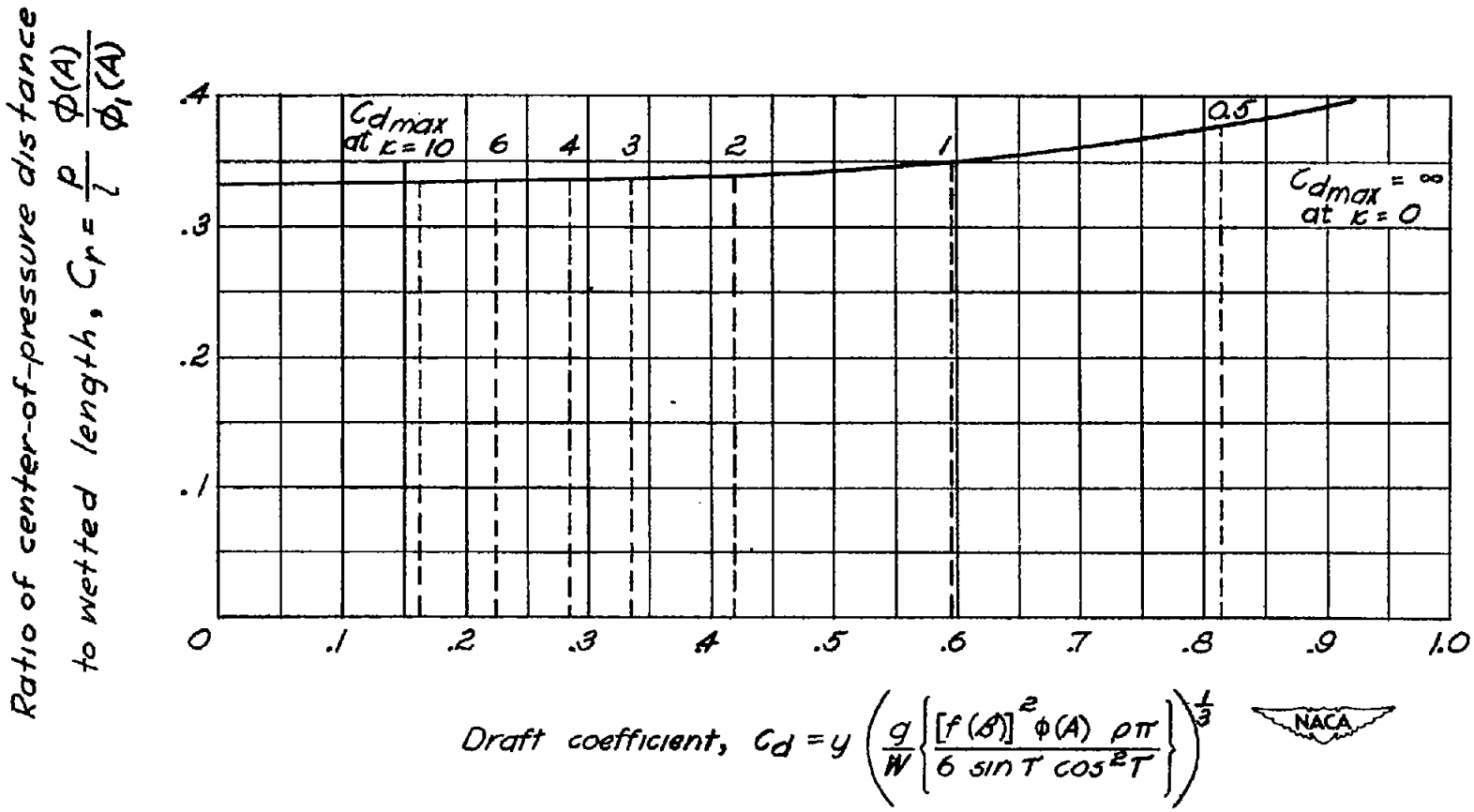

Figure 13. —— Theoretical variation of ratio of center-of-pressure distance to wetted length with draft.

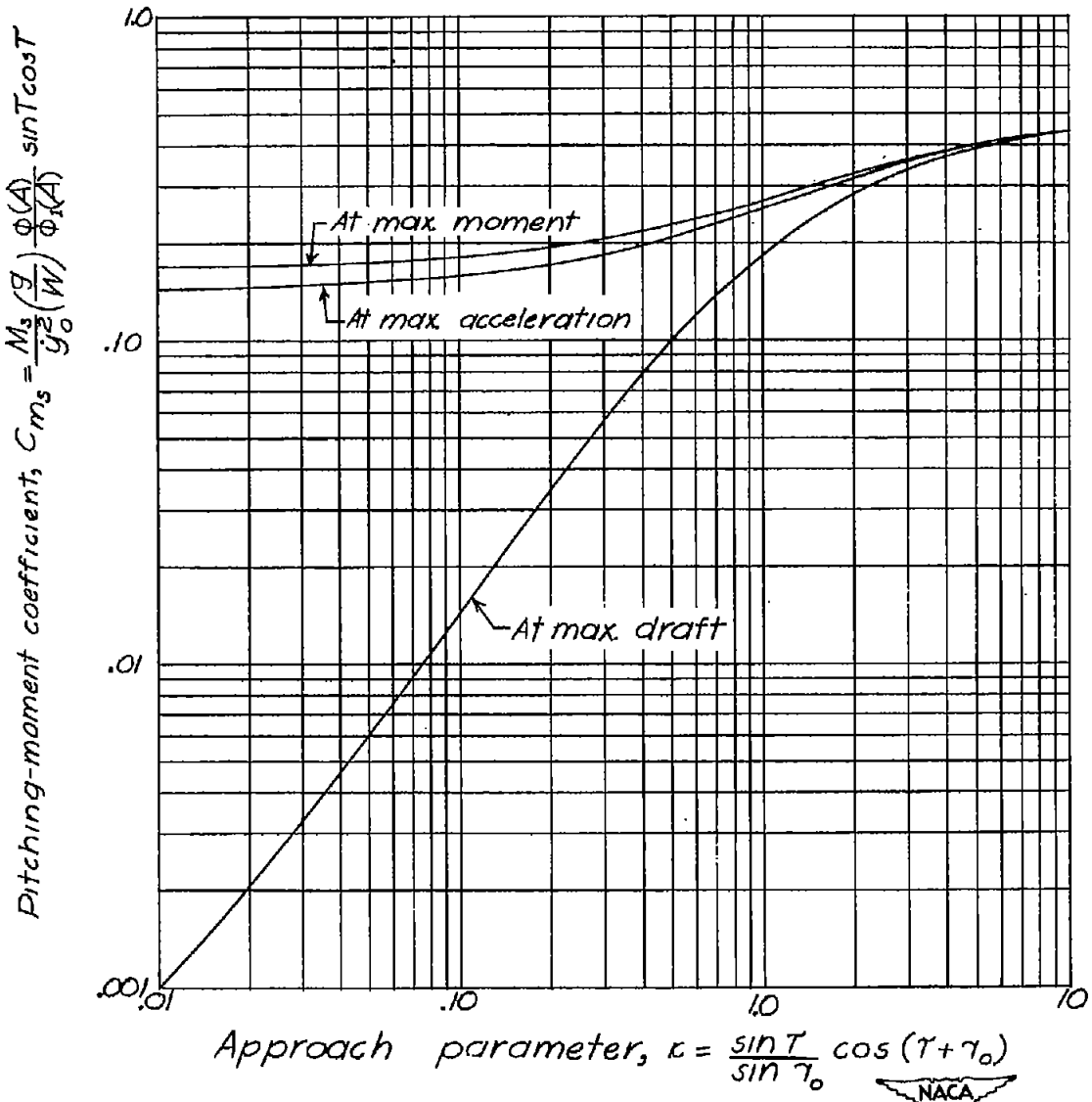

Figure 14.— Theoretical variation of pitching moment at various stages of the impact with approach parameter.

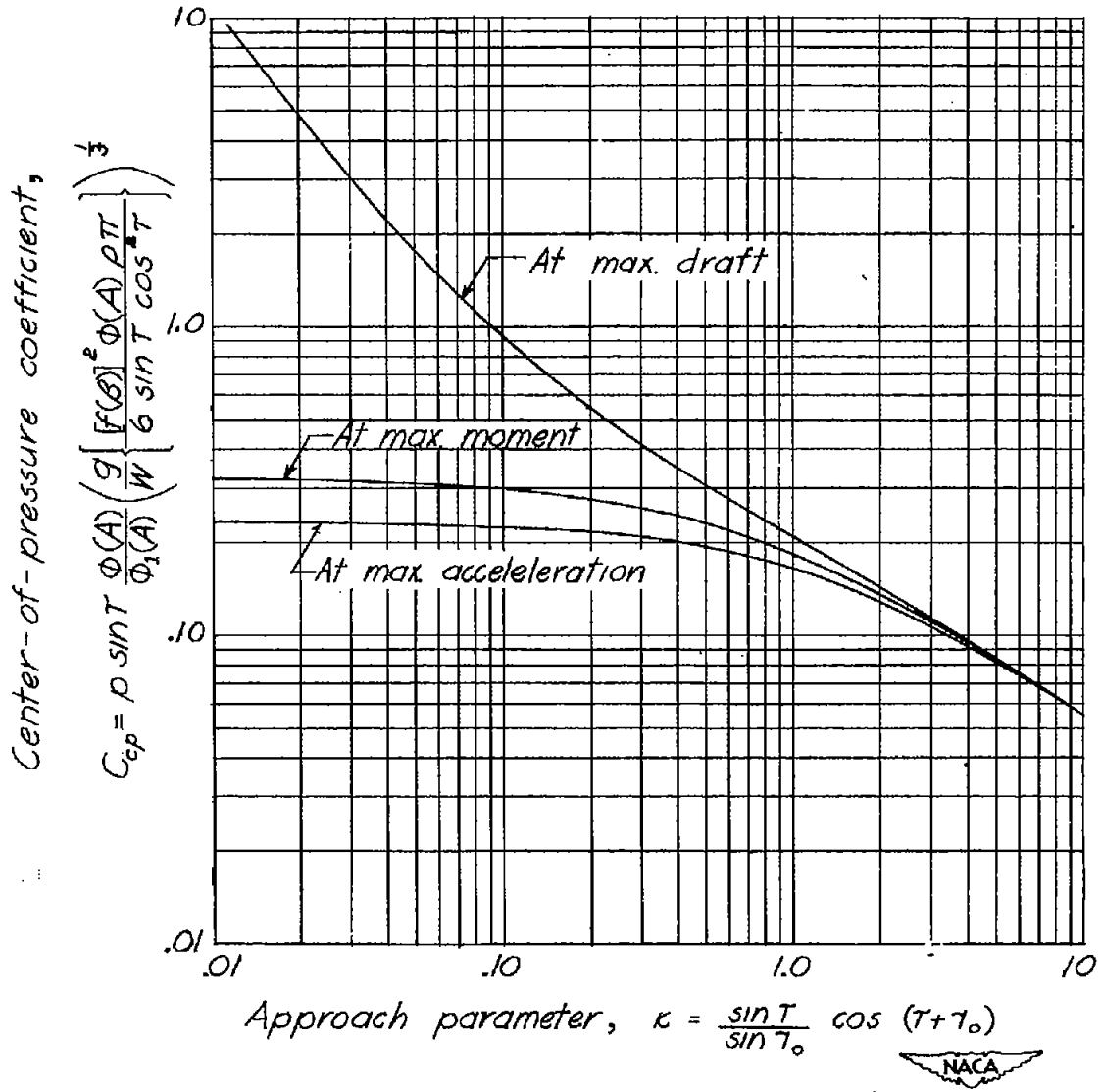

Figure 15. — Theoretical variation of center of pressure at various stages of the impact with approach parameter.

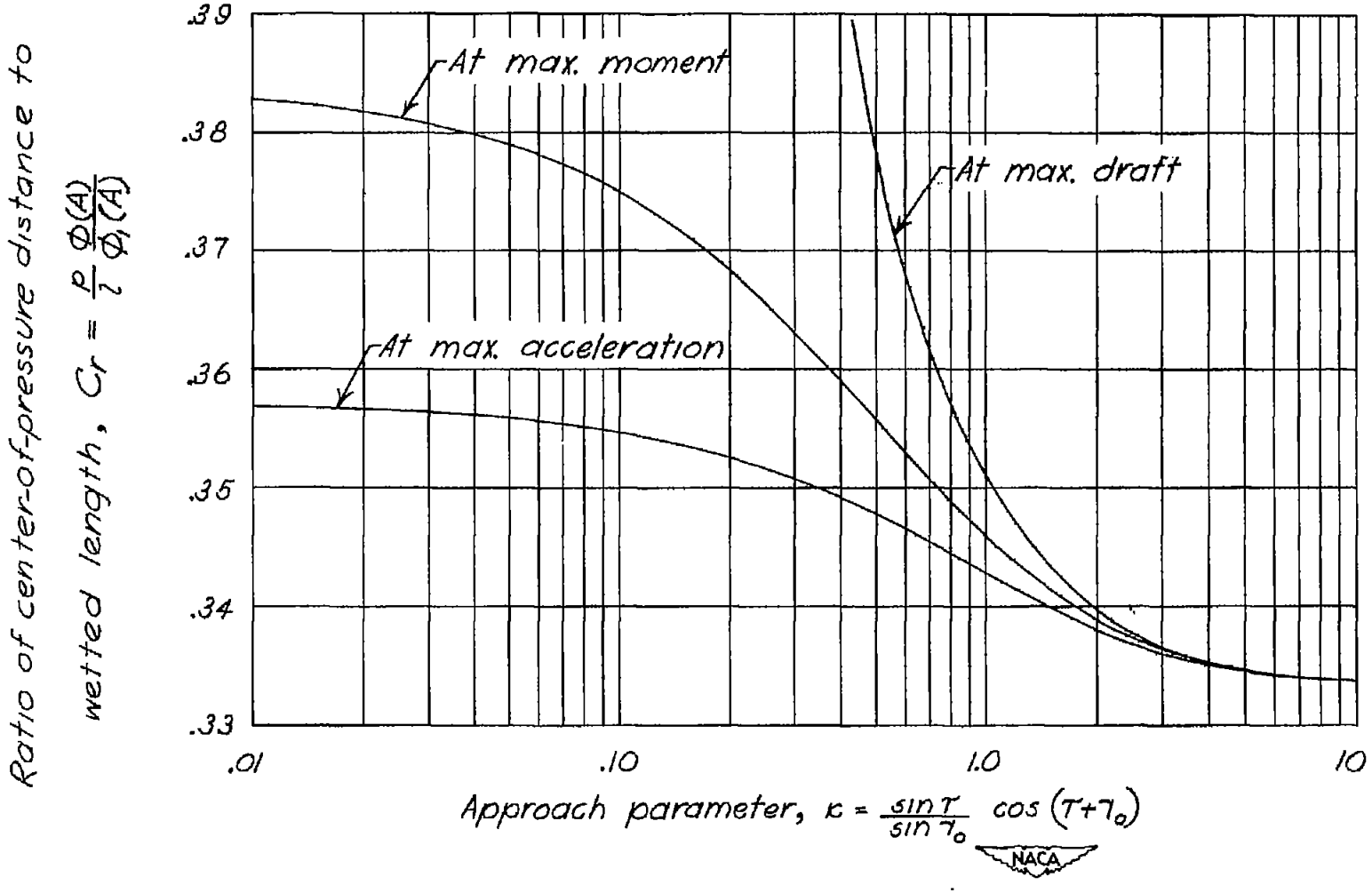

Figure 16.— Theoretical variation of ratio of center-of-pressure distance to wetted length at various stages of the impact with approach parameter.

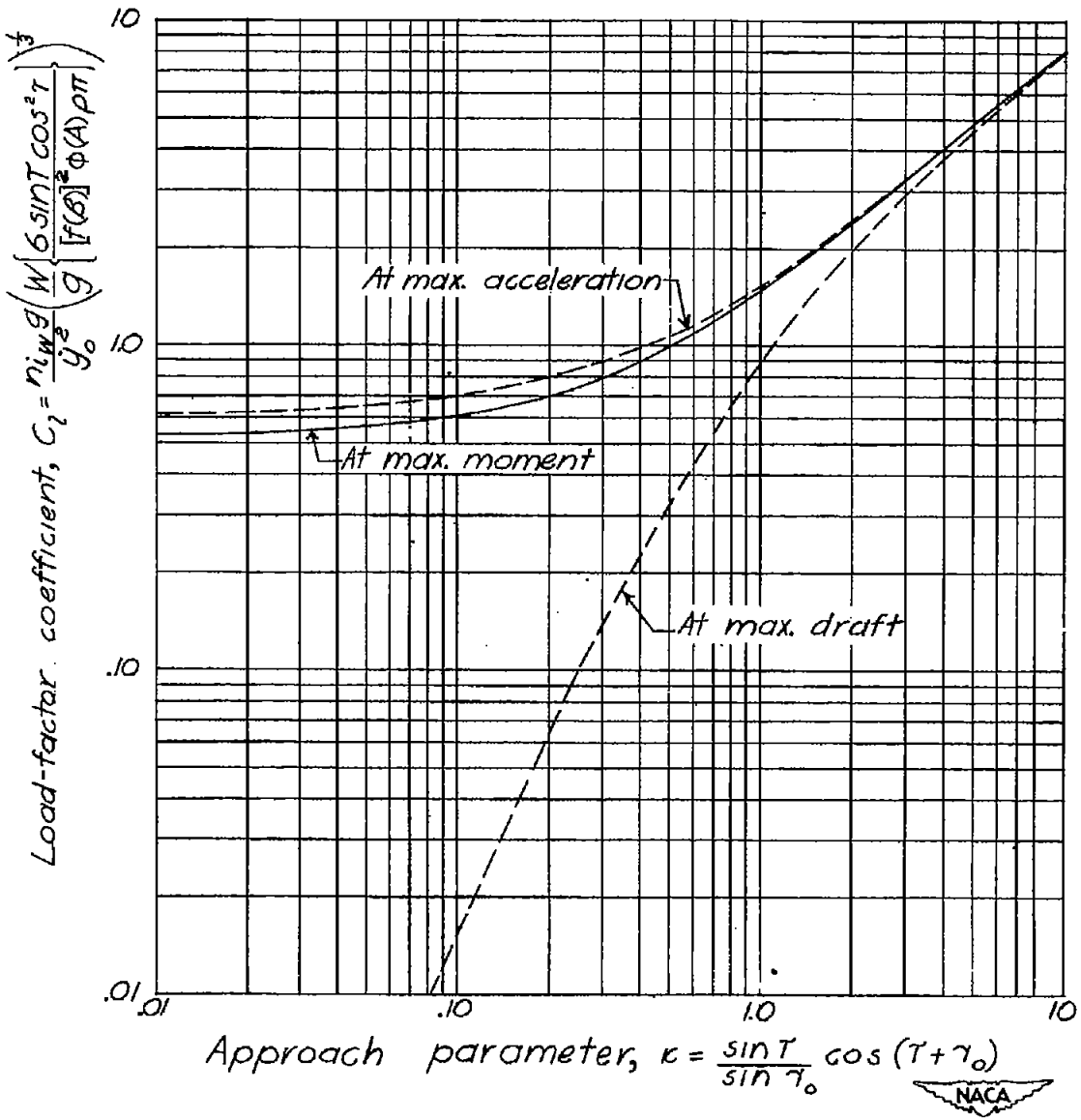

Figure 17.— Theoretical variation of load factor at various stages of the impact with approach parameter.

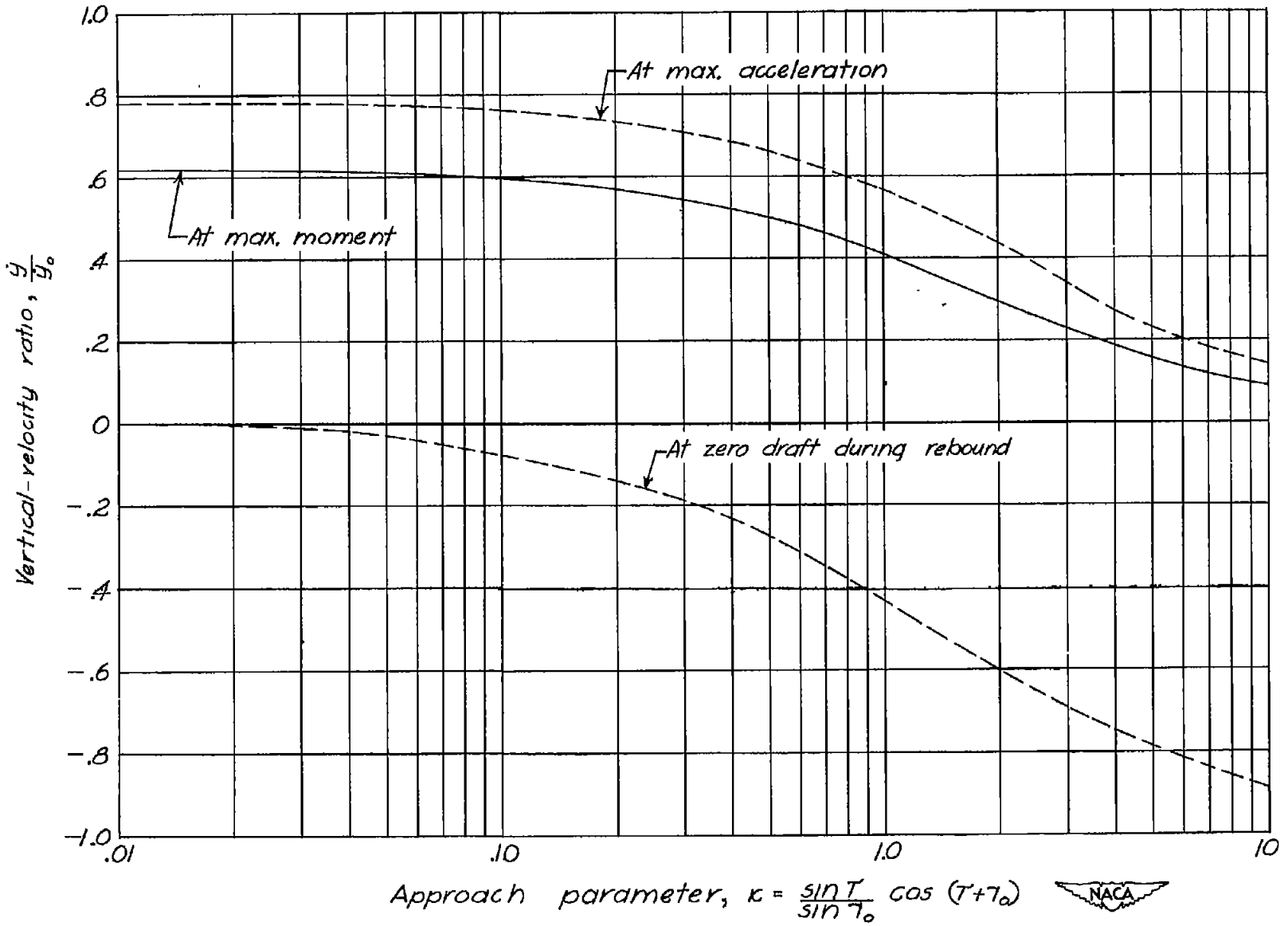

Figure 18.—Theoretical variation of vertical velocity at various stages of the impact with approach parameter.

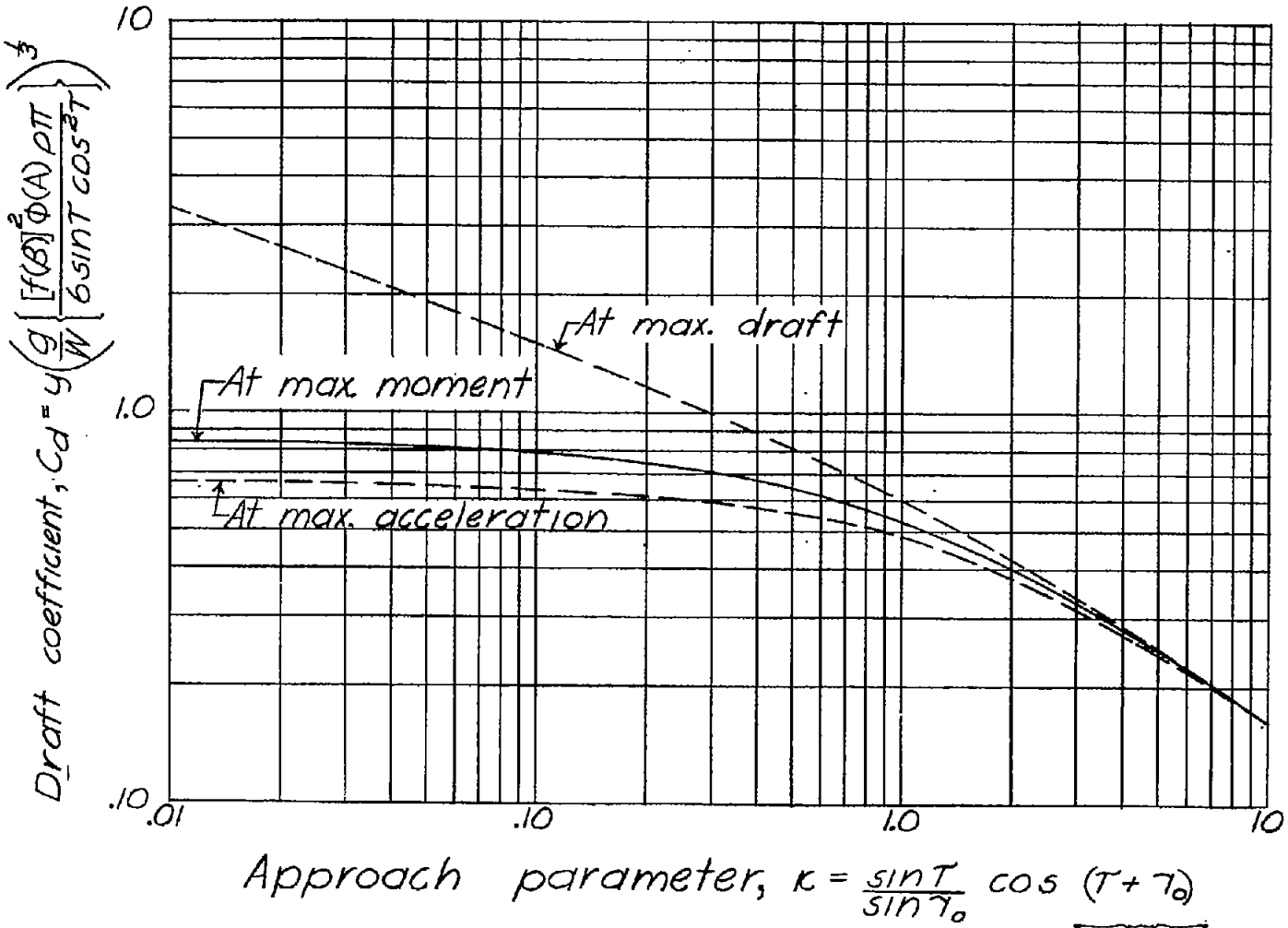

Figure 19.—Theoretical variation of draft at various stages of the impact with approach parameter.

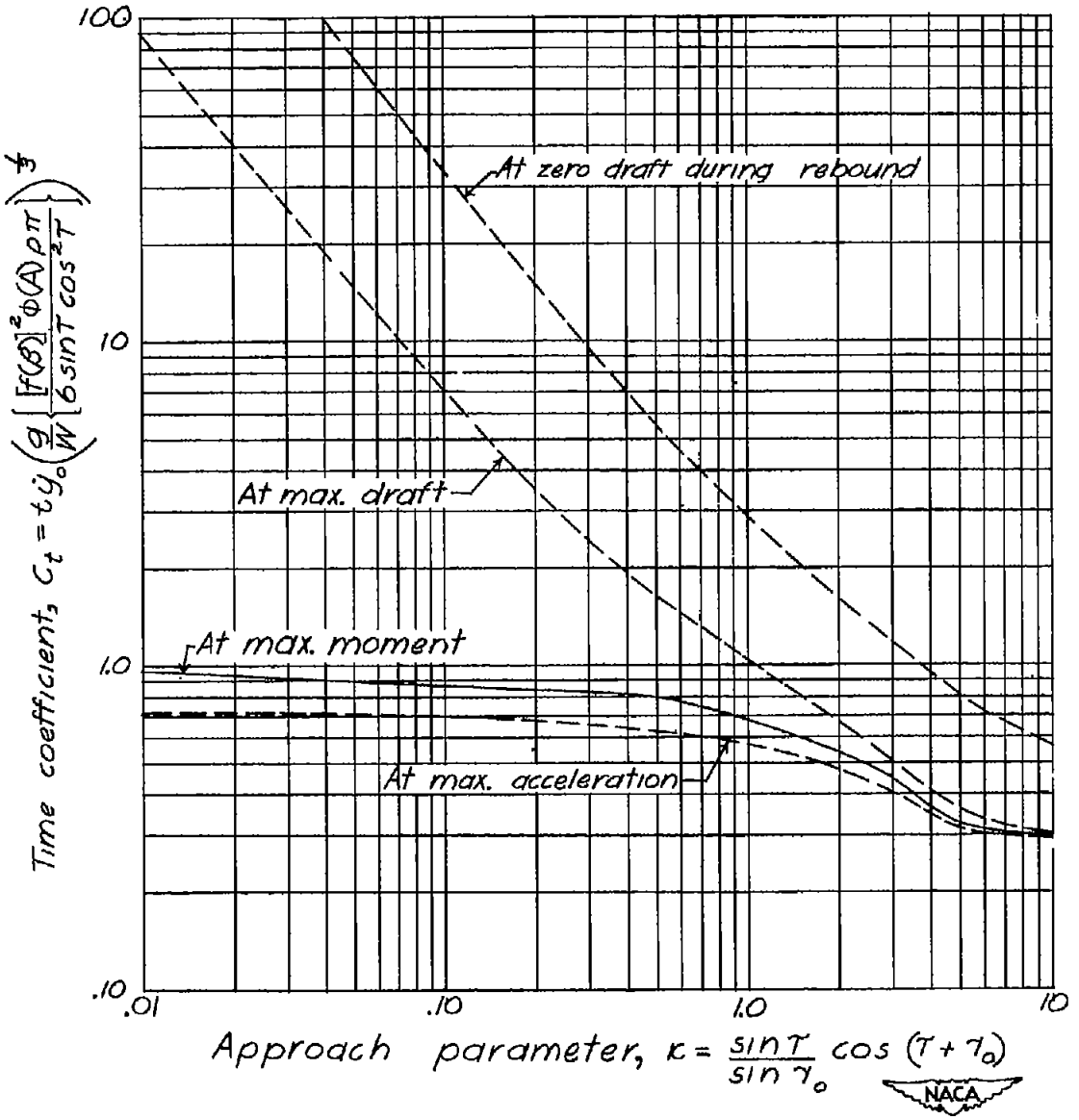

Figure 20.—Theoretical variation of time at various stages of the impact with approach parameter.

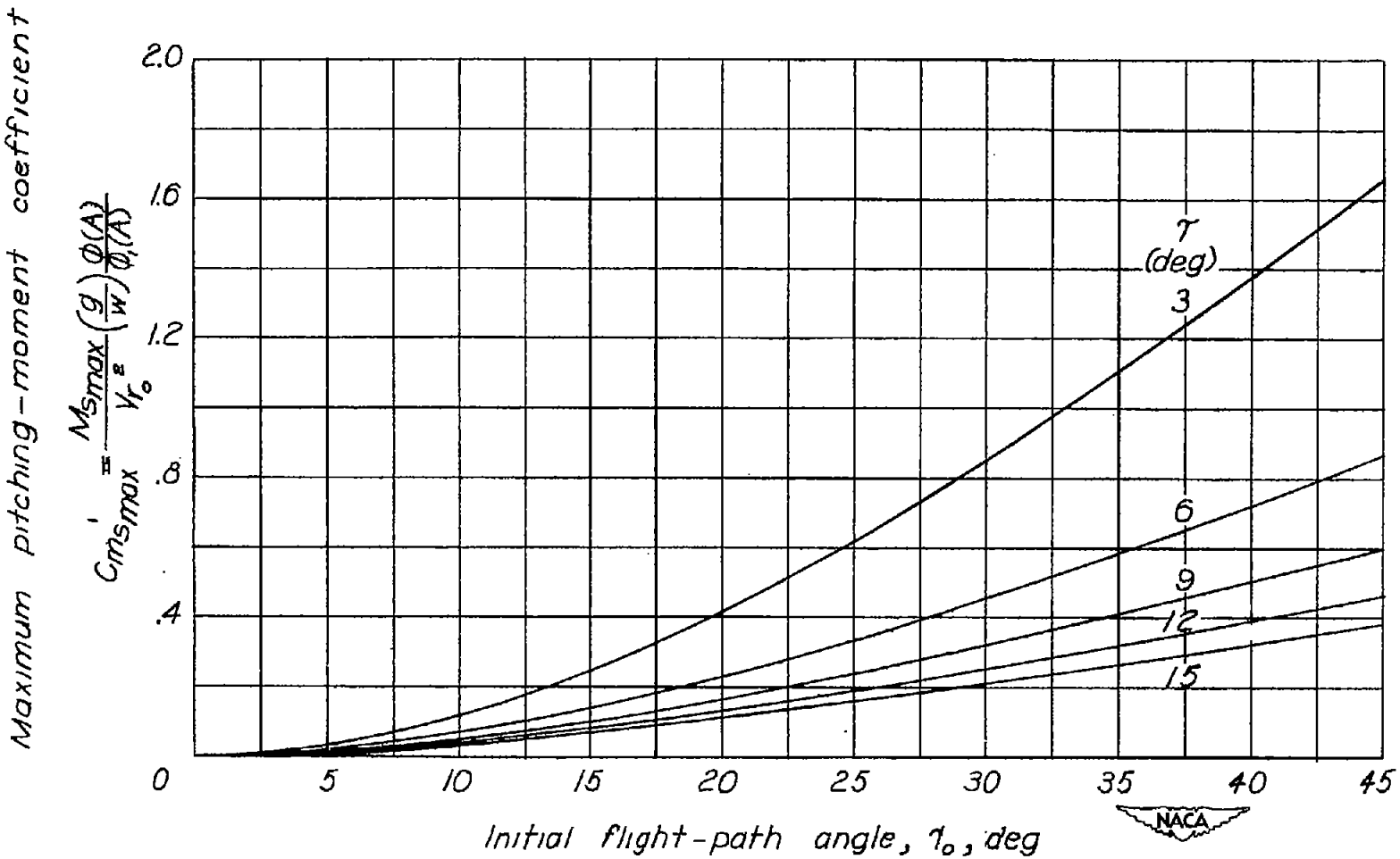

Figure 21.- Theoretical variation of maximum pitching moment with flight-path angle and trim.

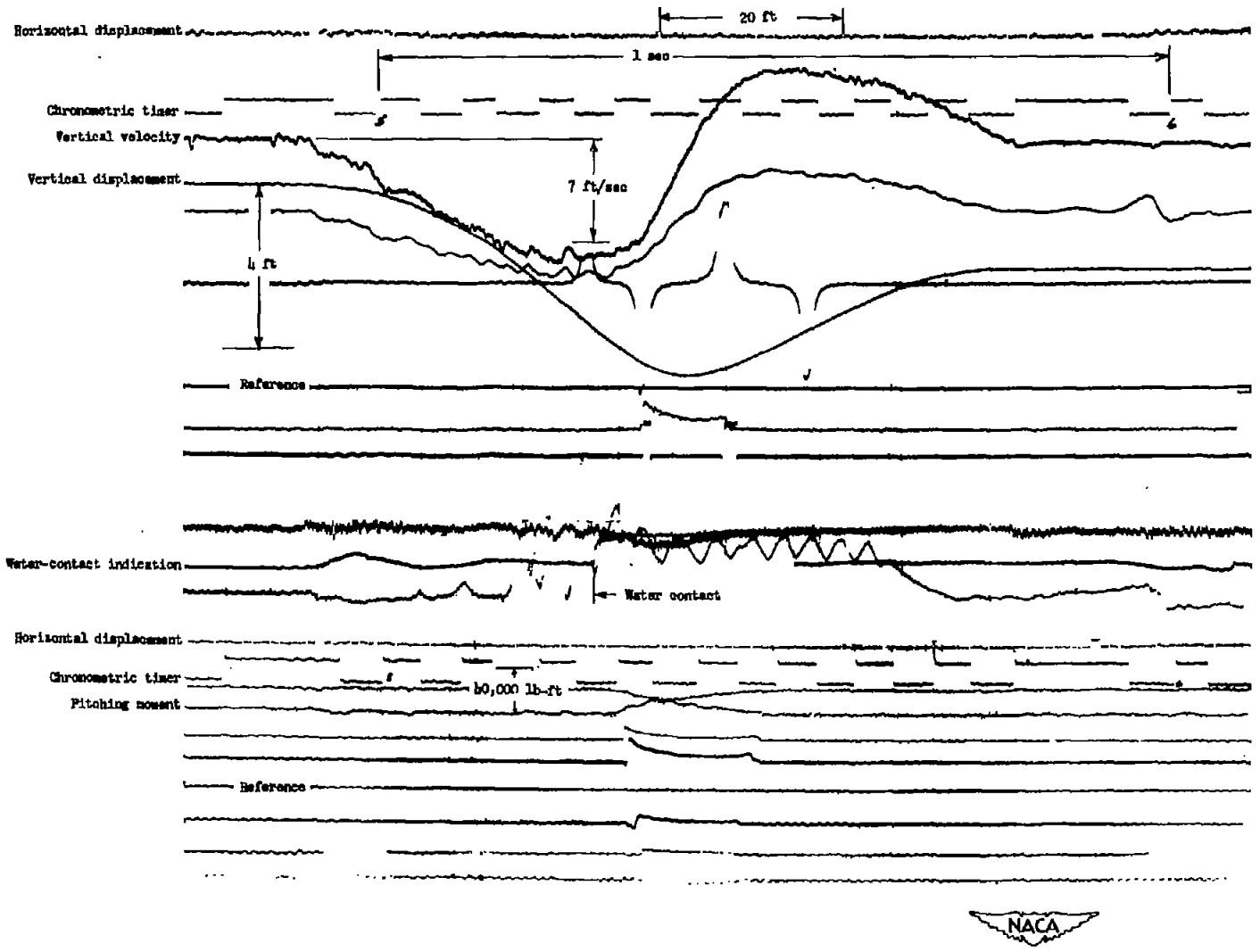

Figure 22.- Typical oscillograph record obtained during tests in the Langley impact basin.

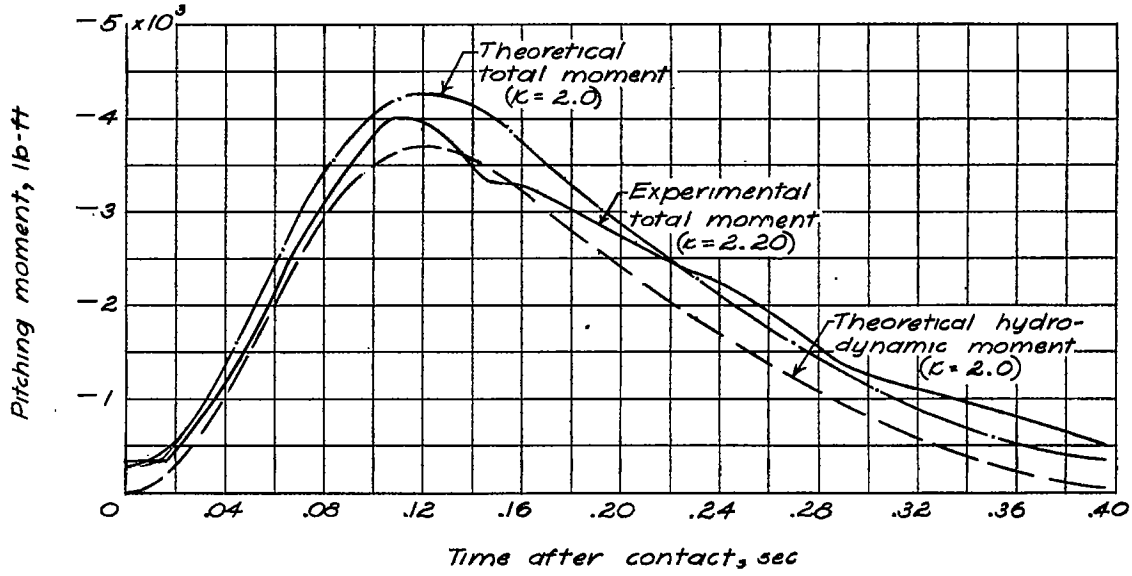

(a) Experimental data: V_{V_0} = 4.95 feet per second; V_{h_0} = 54.55 feet per second; τ_0 = 5.18; k = 2.20.

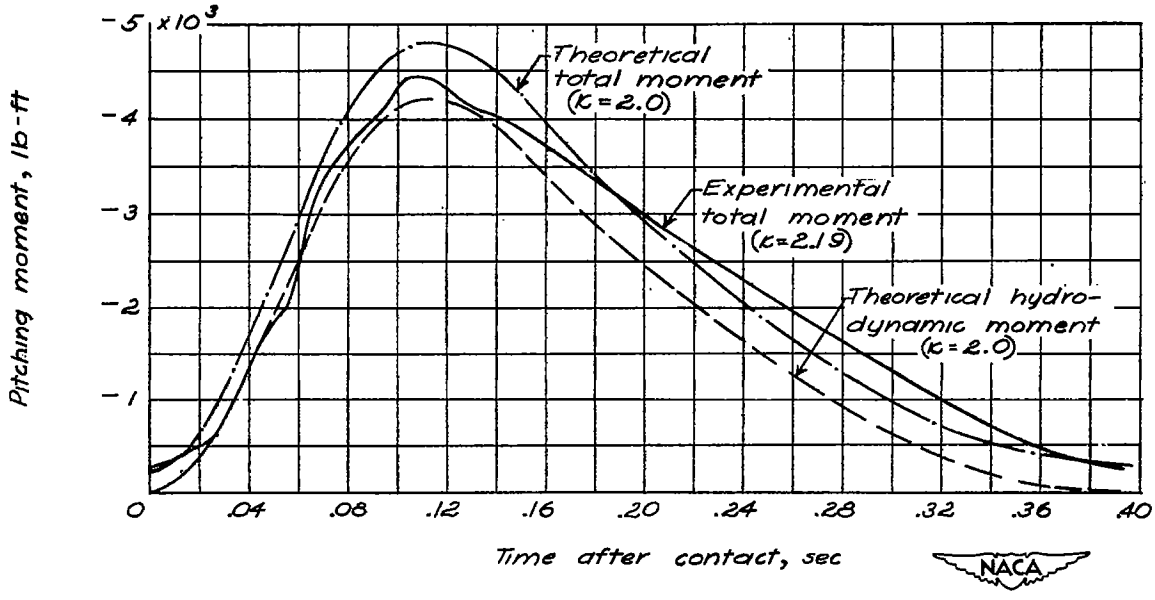

(b) Experimental data: V_{V_0} = 5.28 feet per second; V_{h_0} = 57.89 feet per second; τ_0 = 5.21°; k = 2.19.

Figure 23.— Comparison between theoretical and experimental time histories of pitching moment for a V-bottom seaplane with an angle of dead rise of 30°. W = 1231 pounds; T = 12°.

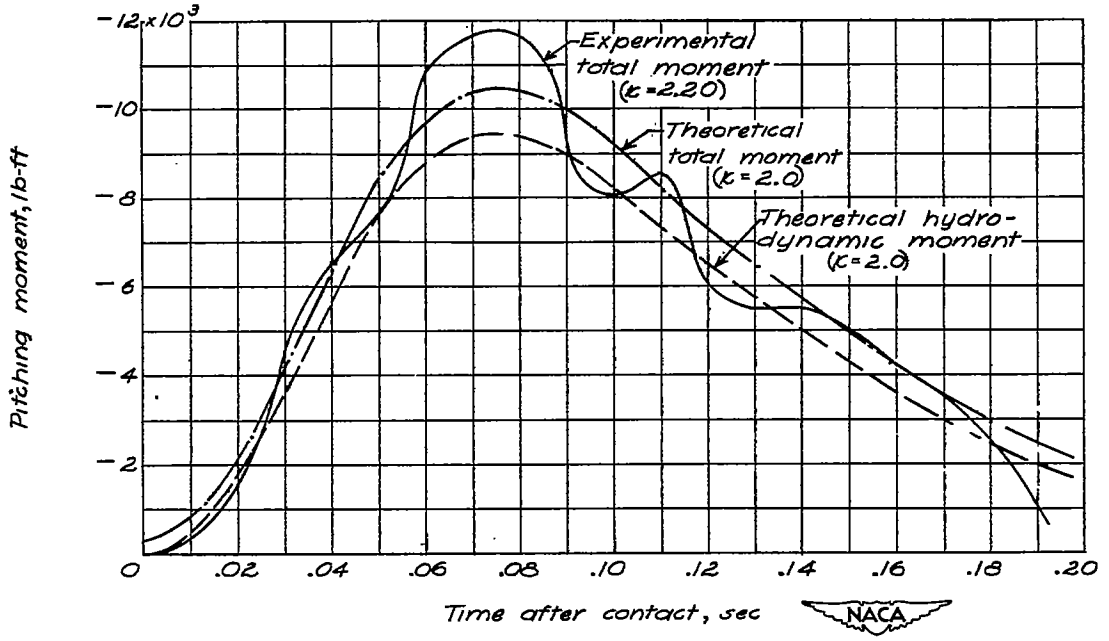

(c) Experimental data: V_{v_0} = 7.92 feet per second; V_{h_0} = 87.50 feet per second; γ_0 = 5.17; κ = 2.20.

Figure 23.— Concluded.

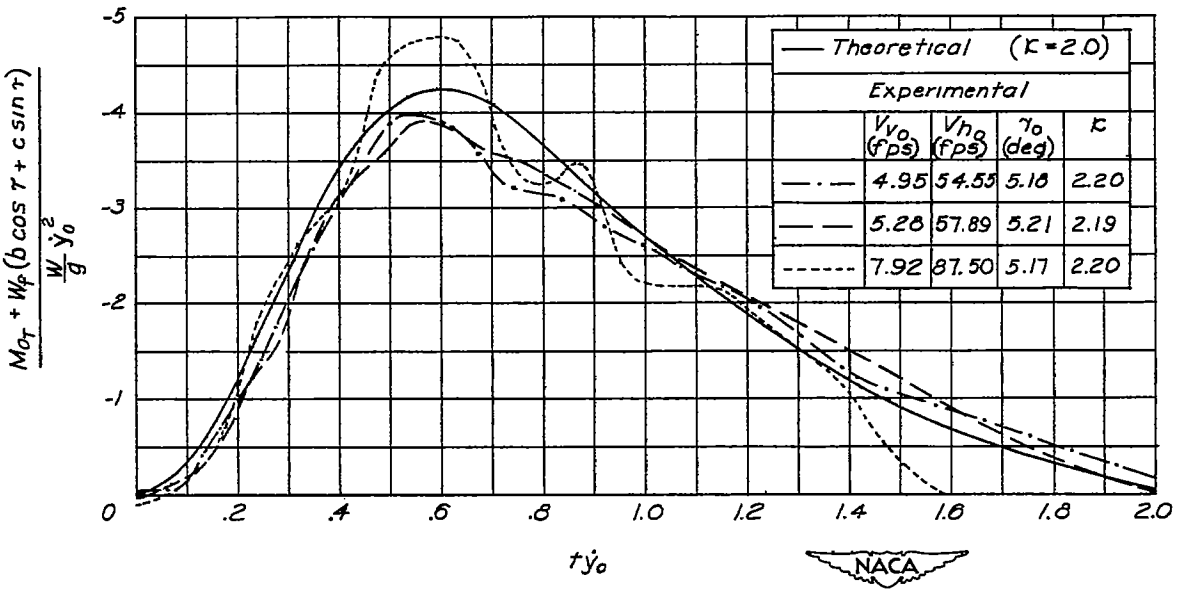

Figure 24.- Comparison of theoretical and experimental variations of total pitching moment for a V-bottom seaplane with an angle of dead rise of 30° and different initial conditions. W = 1231 pounds ; τ = 12°.

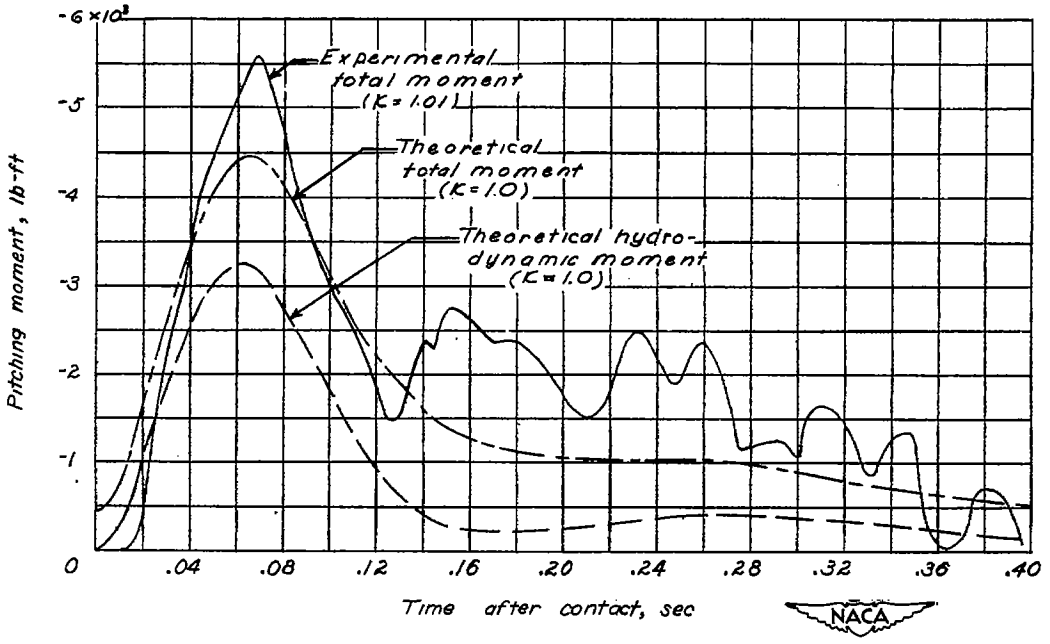

Figure 25.—Comparison between theoretical and experimental time histories of pitching moment for a V-bottom seaplane with an angle of dead rise of 40°. $W = 1213$ pounds; $\tau = 6°$; $V_{V_0} = 8.67$ feet per second; $V_{h_0} = 85.47$ feet per second; $\eta_0 = 5.78°$; $K = 1.0$.

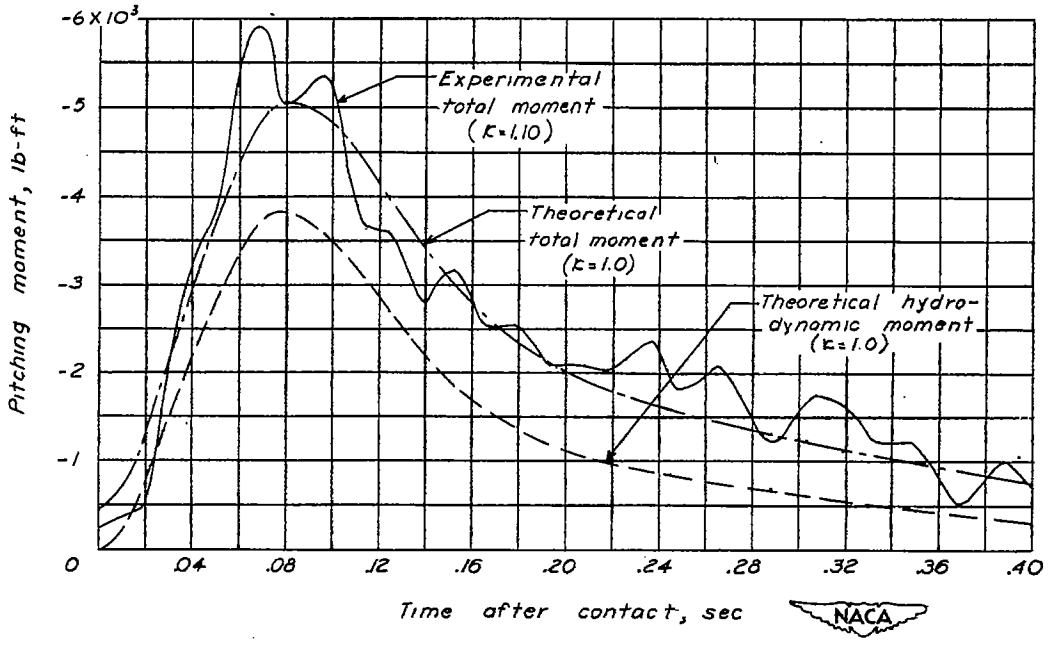

Figure 26.— Comparison between theoretical and experimental time histories of pitching moment for a V-bottom seaplane with an angle of dead rise of 40°. $W = 1213$ pounds; $\tau = 9°$; $V_{V_0} = 8.75$ feet per second; $V_{h_0} = 63.69$ feet per second; $\eta_0 = 7.82°$; $K = 1.10$.

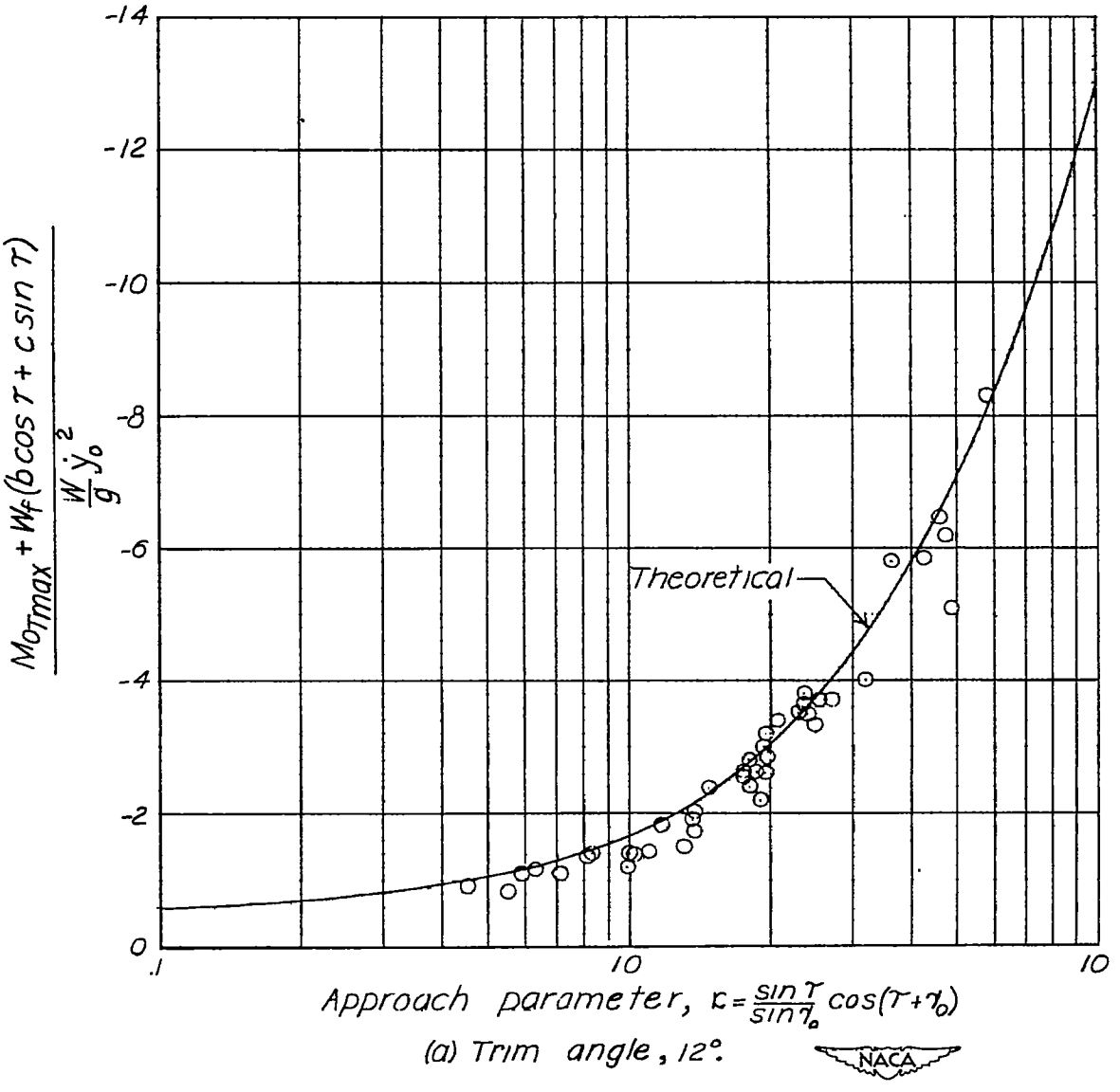

Figure 27.- Comparison between theoretical and experimental variation of maximum total pitching moment with approach parameter. $\beta = 40°$; $W = 1213$ pounds; $W_f = 350$ pounds; $a = 2.89$ feet; $b = 1.05$ feet; $c = 1.81$ feet.

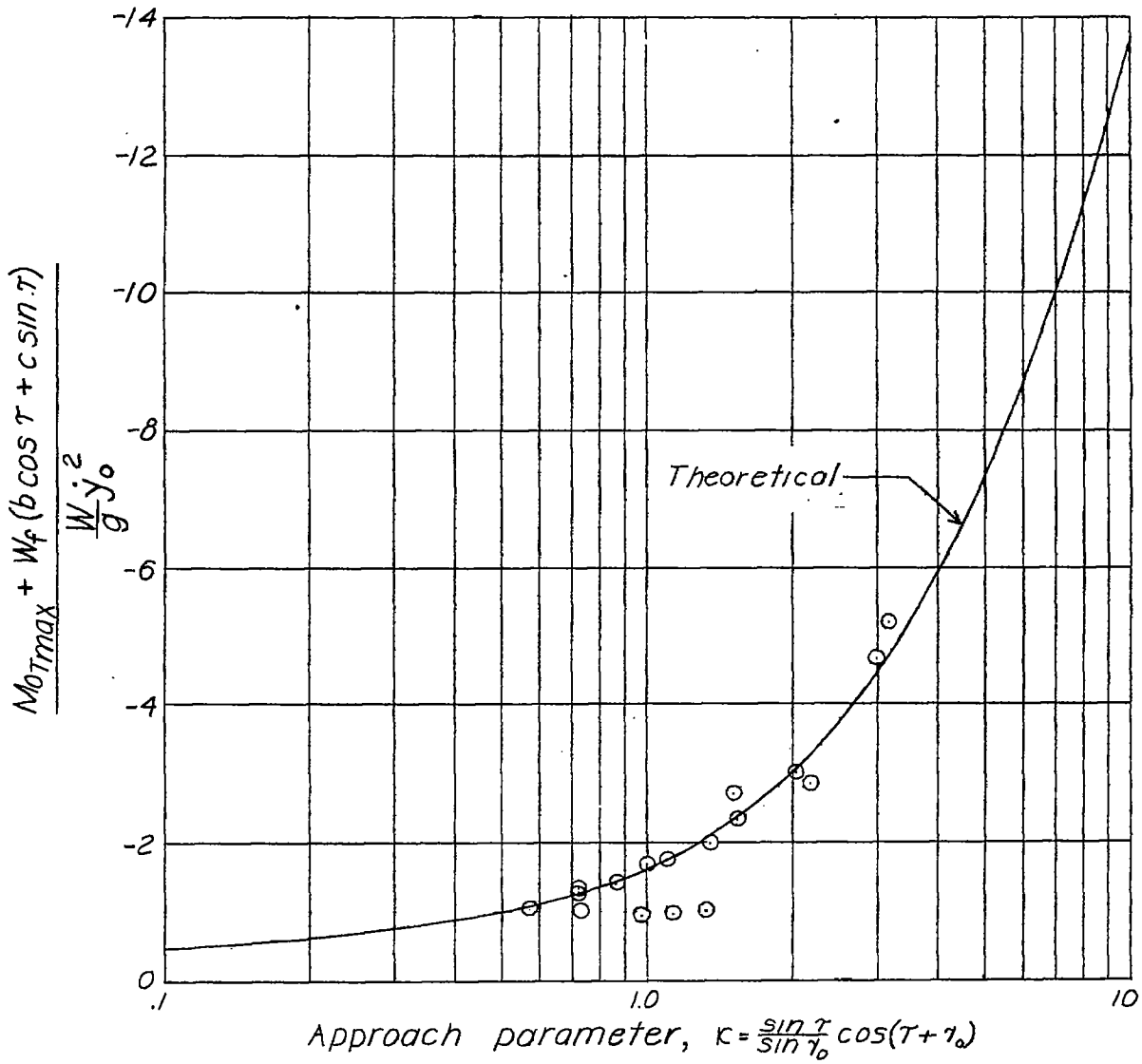

(b) Trim angle, 9°.

Figure 27.- Continued.

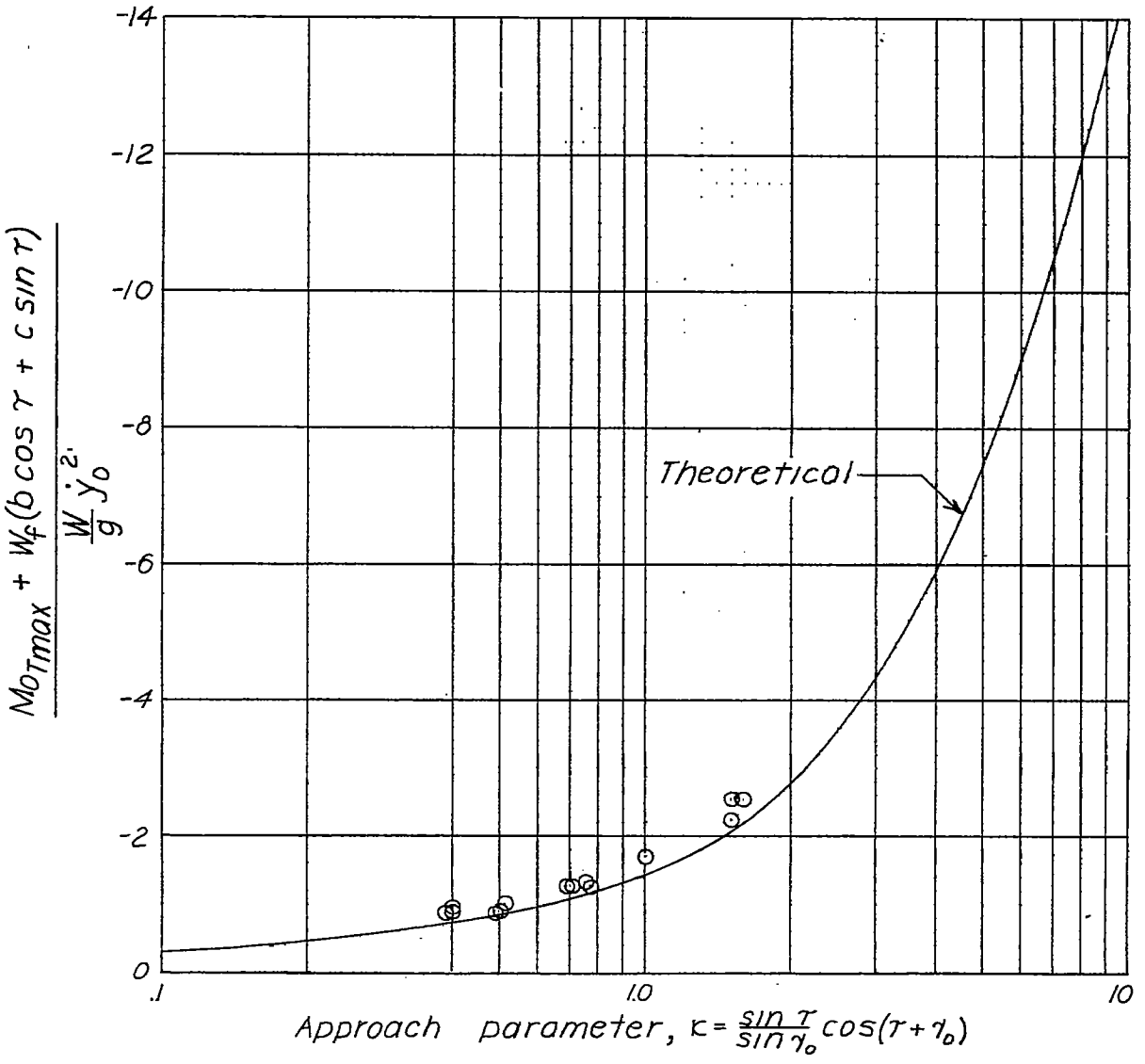

(c) Trim angle, 6°.

Figure 27.- Concluded.

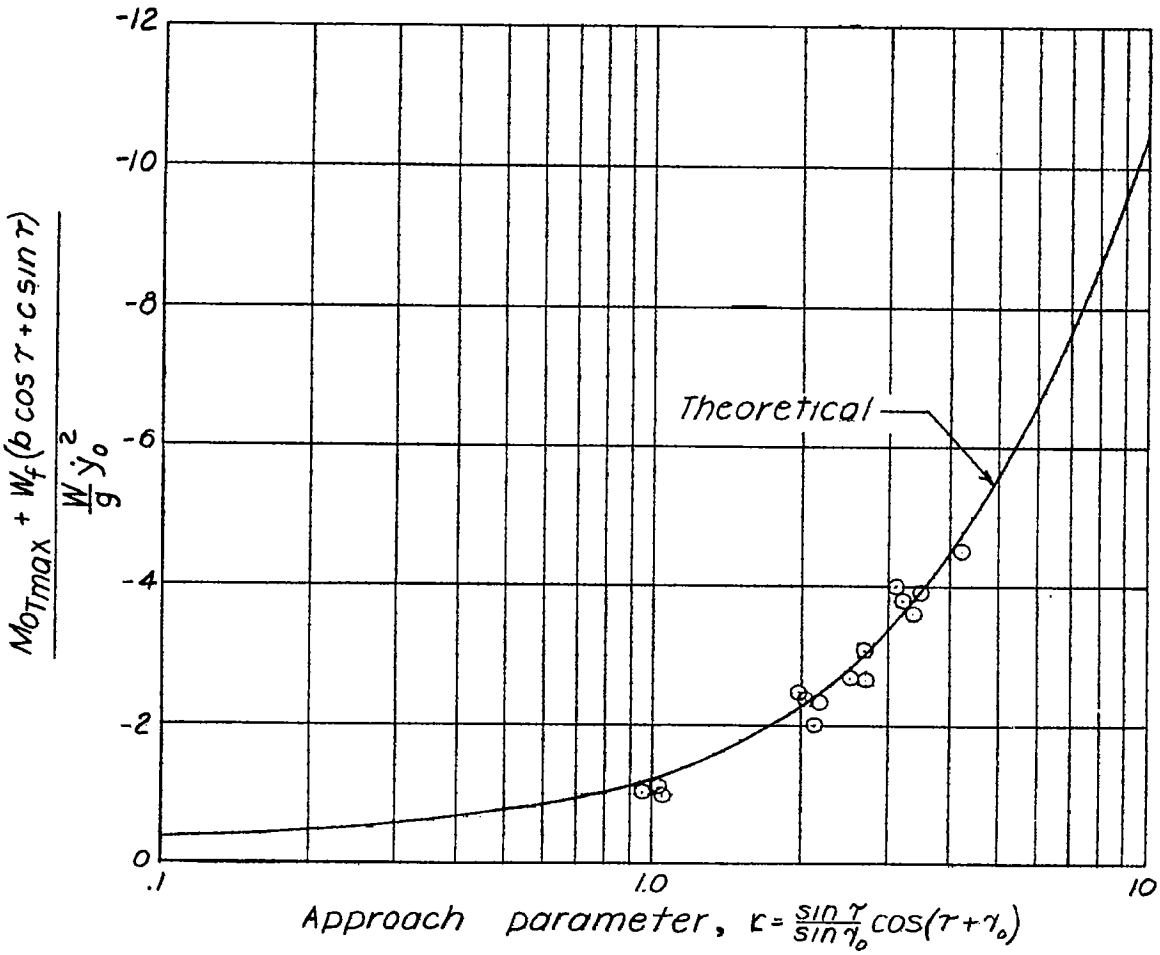

Figure 28.- Comparison between theoretical and experimental variation of maximum total pitching moment with approach parameter. $\beta = 40°$; $\tau = 12°$; $W = 1343$ pounds; $W_f = 590$ pounds; $a = 2.89$ feet; $b = -.28$ feet; $c = 1.46$ feet.